PLANAR DIAGRAM FIELD THEORIES

Gerard 't Hooft

Institute for Theoretical Physics
Princetonplein, 5 P.O. Box 80.006
3508 TA Utrecht, The Netherlands

ABSTRACT

In this compilation of lectures field theories are considered which consist of N component fields q_i interacting with N x N component matrix fields A_{ij} with internal (local or global) symmetry group SU(N) or SO(N). The double expansion in $1/N$ and $\tilde{g}^2 = Ng^2$ can be formulated in terms of Feynman diagrams with a planarity structure. If the mass is sufficiently large and $\tilde{g}^2$ sufficiently small then the (extremely non-trivial) expansion in $\tilde{g}^2$ at lowest order in $1/N$ is Borel summable. Exact limits on the behavior of the Borel integrand for the $\tilde{g}^2$ expansion are derived.

1. INTRODUCTION

In spite of considerable efforts it is still not known how to compute physical quantities reliably and accurately in any four-dimensional field theory with strong interactions. It seems quite likely that if any strong interaction field theory exists in which accurate calculations can be done, then that must be an asymptotically free non-Abelian gauge theory. In such theories the small-distance structure is completely described by solutions of the renormalization group equations[1]; and there are reasons to believe that the continuum theory can be uniquely defined as a limit of a lattice gauge theory[2], when the size of the meshes of the lattice tends to zero, together with the coupling constant, in a way prescribed by this renormalization group[3]. Indeed, one can prove using this formalism[4] that this limit exists up to any finite order in the perturbation expansion for small coupling.

However, this result has not been extended beyond pertur-

bation expansion. It is important to realize that this might imply that theories such as "quantum chromodynamics" (QCD) are not based on solid mathematics, and indeed, it could be that physical numbers such as the ratio between the proton mass and the string constant do not follow unambiguously from QCD alone. In view of the qualitative successes of the recent Monte-Carlo computation techniques[5] the idea that hadronic properties could be shaped by forces other than QCD alone seems to be far-fetched, but it would be extremely important if this happened to be the case. More likely, we may simply have to improve our mathematics to show that QCD is indeed an unambiguous theory. Either way, it will be important to extend our understanding of the summability aspects of higher order perturbation theory as well as we can. The following constitutes just such an attempt.

There are two categories of divergences when one attempts to sum or resum perturbation expansion for a field theory in four space-time dimensions. One is simply the divergence due to the increasingly large numbers of Feynman diagrams to consider at higher orders. They grow roughly as n! at order g^{2n}. This is a kind of divergence that already occurs if the functional integral is replaced by some ordinary finite-dimensional integral of similar type:

$$I(g^2) = \int d\vec{\phi} \; e^{-S(\vec{\phi})} \; ,$$

$$S(\vec{\phi}) = \tfrac{1}{2}(\vec{\phi},M\vec{\phi}) + g \sum A_{ijk}\phi_i\phi_j\phi_k$$
$$+ g^2 \sum B_{ijk\ell}\phi_i\phi_j\phi_k\phi_\ell \; . \qquad (1.1)$$

Here the diagrams themselves are bounded by geometric expressions but the numbers K(n) of diagrams of order n are such that the expansion is only asymptotic:

$$I(g^2) \rightarrow \sum_n K(n) \; C^n \; g^{2n} \; ;$$

$$K(n) \rightarrow a^n \; n! \qquad , \qquad (1.2)$$

where a is determined by one of the stationary points of the action S, called "instantons".

However in four-dimensional field theories the diagrams themselves are not geometrically bounded. In some theories it has been shown[6] that diagrams of the nth order that required k ultra-violet subtractions (with essentially $k \lesssim n$) can be bounded at best by

$$b^n k! g^{2n} . \qquad\qquad (1.3)$$

But since the total number of such diagrams grow at most as $n!/k!$ we still get bounds of the form (1.2) for the total amplitude, however with a replaced by a different coefficient. This is a different kind of divergence sometimes referred to as ultraviolet "renormalons"[4,7].

If a field theory is asymptotically free the corresponding coefficient b is negative and one might hope that the ultraviolet renormalons are relatively harmless. But in massless theories a similar kind of divergence will then be difficult to cope with: the infrared renormalons, which, as the word suggests, are due to a build-up of infrared divergences at very high orders: individual diagrams may still be convergent but their sum diverges again with $n!$ The theories we will study more closely are governed by planar diagrams only. Their numbers grow only geometrically[8] so that divergences due to instantons are absent. These diagrams are akin to but more complicated than Bethe-Salpeter ladder diagrams and by trying to sum them we intend to learn much about the renormalon divergences.

Infinite color quantum chromodynamics is of course the most interesting example of a planar field theory but unfortunately our analysis cannot yet be carried out completely there. We do get bounds on the behavior of its Borel functions however (sect. 17).

Examples of large N field theories that we can handle our way are given in sect. 3 and appendix A.

2. FEYNMAN RULES FOR ARBITRARY N

In order to show that the set of planar Feynman diagrams becomes dominant at large N values we first formulate a generic theory at arbitrary N, with a coupling constant g as expansion parameter in the usual sense.

Let us express the fields as a finite number K of N-component vectors $\psi_i^a(x)$ ($a=1,\ldots,K$; $i=1,\ldots,N$), and a small number D of N x N matrices $A^b{}_i{}^j(x)$, where $b=1,\ldots,D$ and $i,j=1,\ldots,N$. Usually we will take ψ to be complex and $A_i{}^j$ to be Hermitean, in which case thesymmetry group will be U(N) or SU(N). The case that ψ_i are real and $A_i{}^j$ real and symmetric can easily be included after a few changes, in which case the symmetry group would be O(N) or SO(N), but the complex case seems to be more interesting from a physical point of view. In quantum chromodynamics K would be proportional to the number of flavors and D is the number of space-time dimensions plus two for the (non-Hermitean) ghost field.

In general then the Lagrangian has the form

$$\mathcal{L}(A,\psi,\psi^*) = - \sum_{a,...} \psi^{*a}\left(M_0^{ab} + gM_1^{abc}A^c + \tfrac{1}{2}g^2M_2^{abcd}A^cA^d\right)\psi^b$$

$$- \mathrm{Tr}\left(\tfrac{1}{2}R_0^{ab}A^aA^b + \tfrac{1}{3}gR_1^{abc}A^aA^bA^c + \tfrac{1}{4}g^2R_2^{abcd}A^aA^bA^cA^d\right), \qquad (2.1)$$

with

$$A^a{}_i{}^j = \left(A^a{}_j{}^i\right)^*. \qquad (2.2)$$

Here the usual matrix multiplication rule with respect to the indices $i,j,...$ is implied, and Tr stands for trace with respect to these indices. The objects M and R carry no indices i,j but only "flavor" indices $a,b,...$. Furthermore $M_{0,1}$ and $R_{0,1}$ may contain the derivatives of $\psi(x)$ or $A(x)$. So the case that ψ are fermions is included: then $a,b,...$ may include spinor indices. The coupling constant g has been put in (2.1) in such a way that it is a handy expansion parameter.
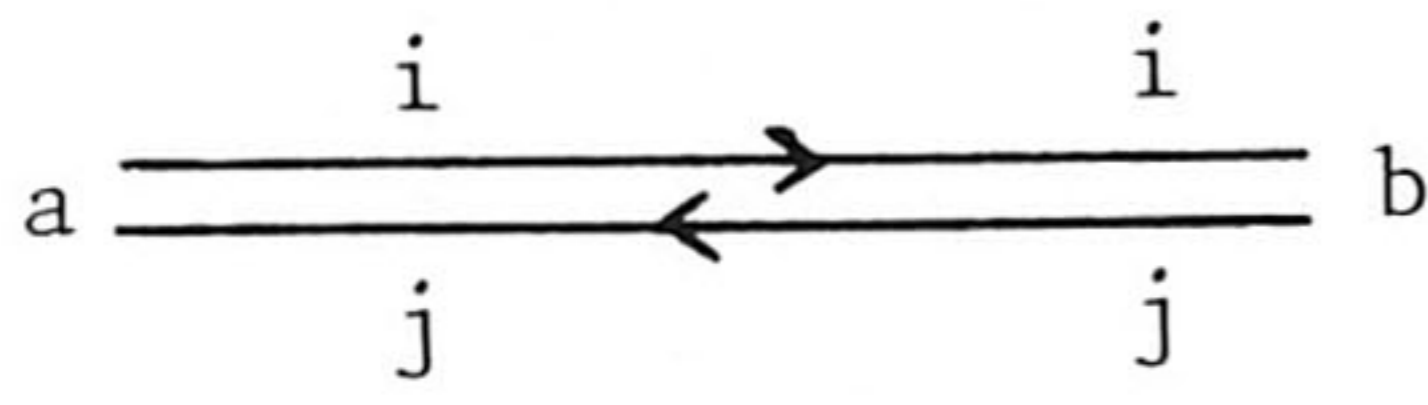
In order to keep track of the indices $i,j,...$ it is convenient to split the fields $A^a{}_i{}^j$ into complex fields for $i > j$ and real fields for $i = j$. One can then denote an upper index by an incoming arrow and a lower index by an outgoing arrow. The propagator is then denoted by a double line. In fig. 1, the A propagator stands for an $A_i{}^j$ propagator to the right if $i > j$; an $A_j{}^i$ propagator to the left if $i < j$ and a real propagator if $i = j$.

It is crucial now that the coefficients M and P in the Lagrangian respect the U(N) (or O(N)) symmetry: they carry no indices $i,j,...$. Hence the vertices in the Feynman graphs only depend on these indices *via* Kronecker deltas. We indicate such a Kronecker delta in a vertex by connecting the corresponding index lines. Since we have a unitary invariance group these Kronecker deltas only connect upper indices with lower indices, therefore the index lines carry an *orientation* which is preserved at the vertices. This is where the unitary case differs from the real orthogonal groups: the restriction to real fields with O(N) symmetry corresponds to dropping the arrows in Fig. 1: the index lines then carry no orientation.
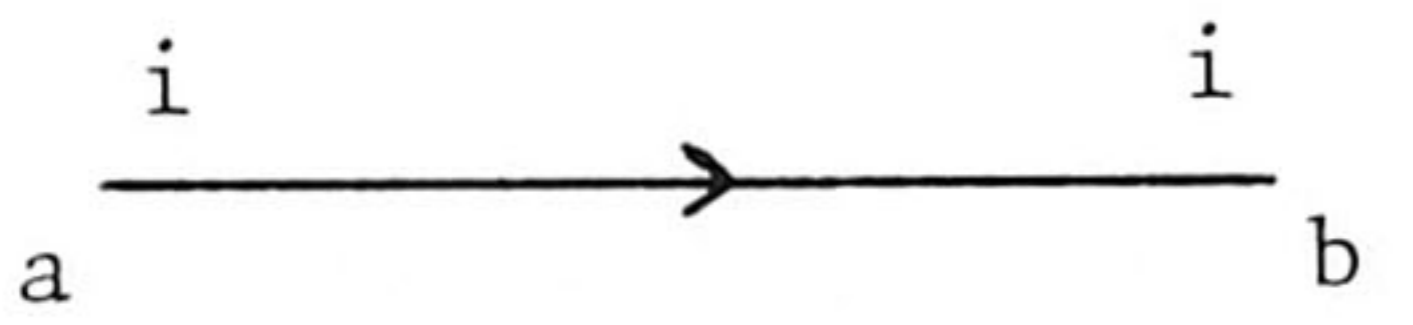
As for the rest the Feynman rules for computing a diagram are as usual. For instance, fermionic and ghost loops are associated with extra minus signs.

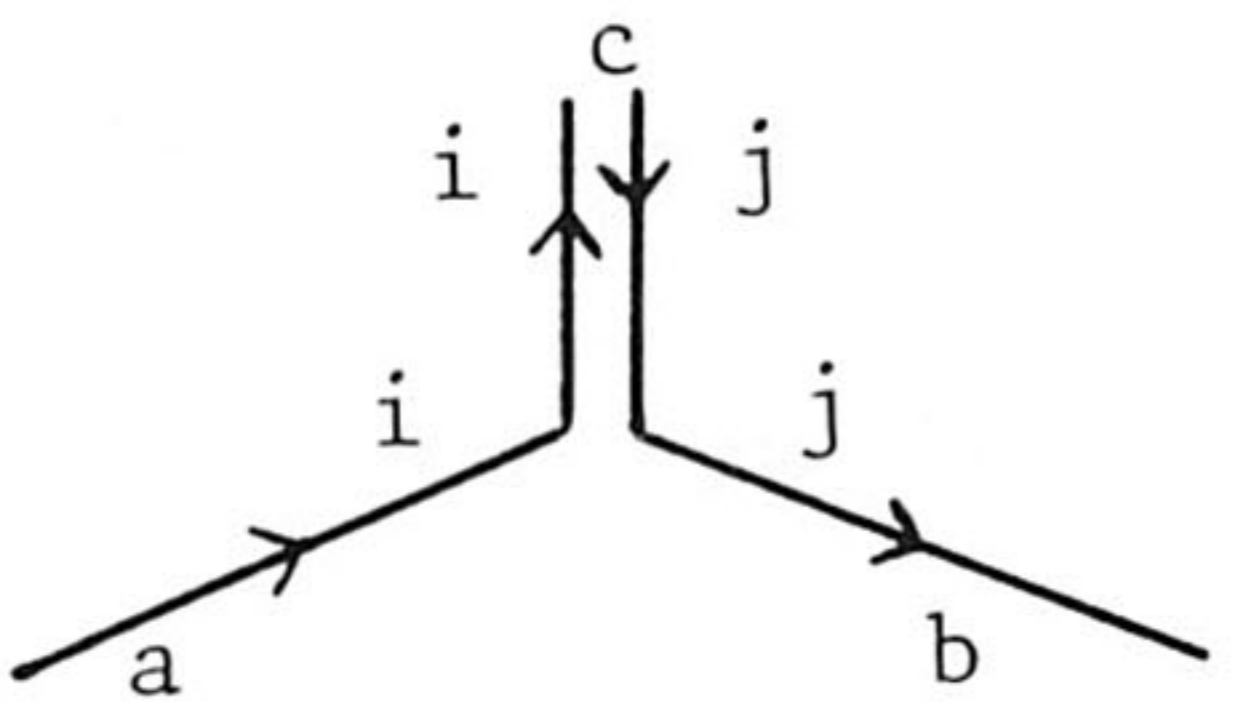In some theories (such as SU(N) gauge theories) we have an extra constraint:

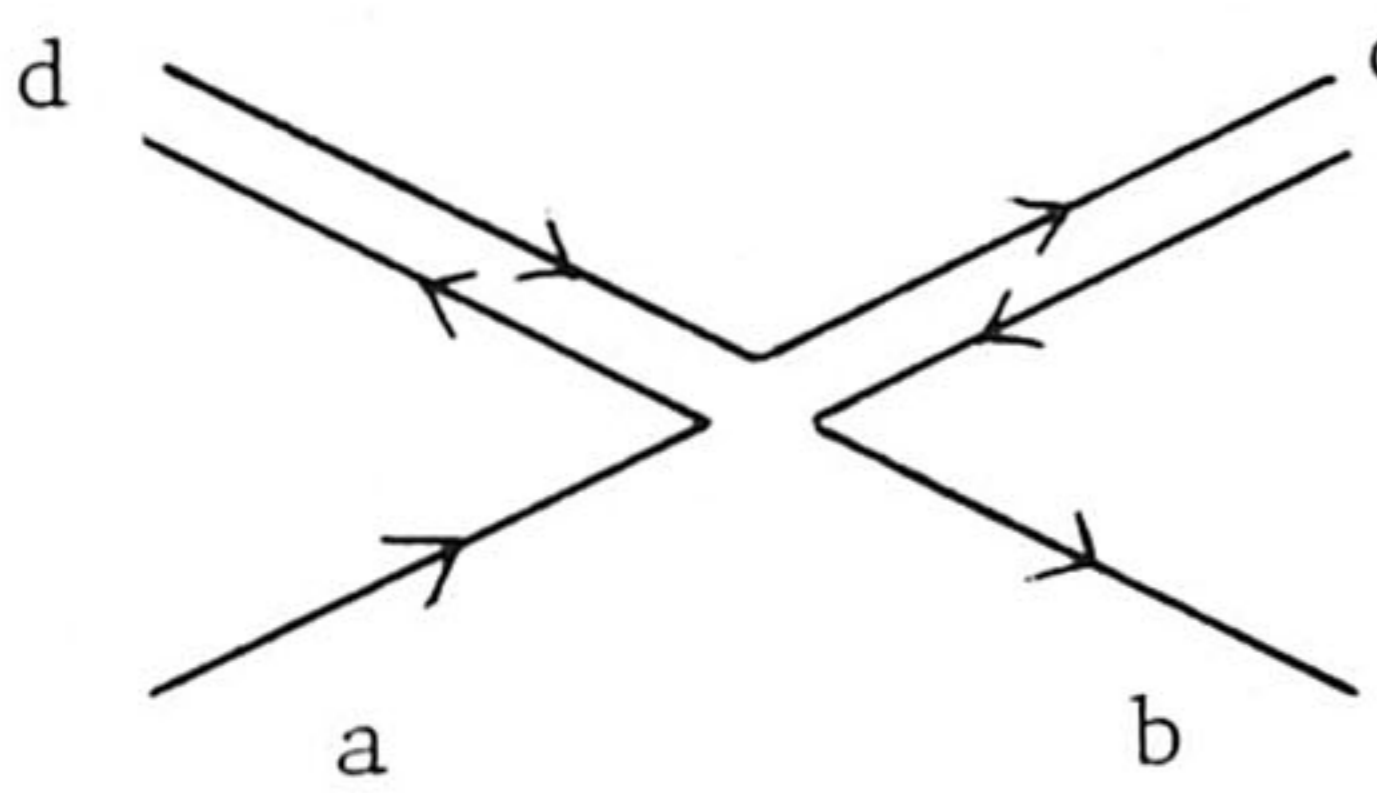$$\mathrm{Tr}\ A^a = 0. \qquad (2.3)$$

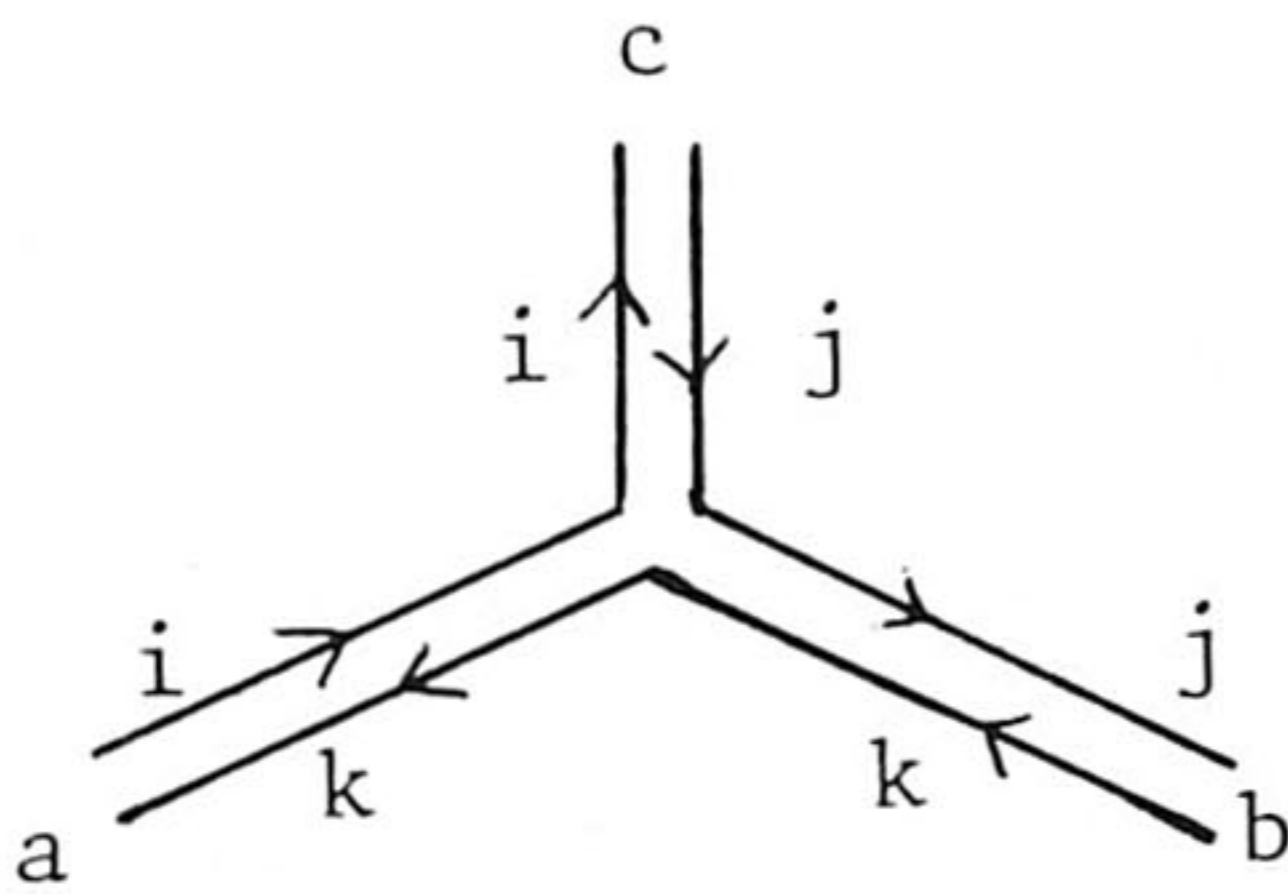$$P_{ab}(k) = \{R_o\}^{-1}_{ab} \quad \text{(N x N matrix propagator)}$$

$$P'_{ba}(k) = (M_o^{-1})_{ba} \quad \text{(N-vector propagator)}$$
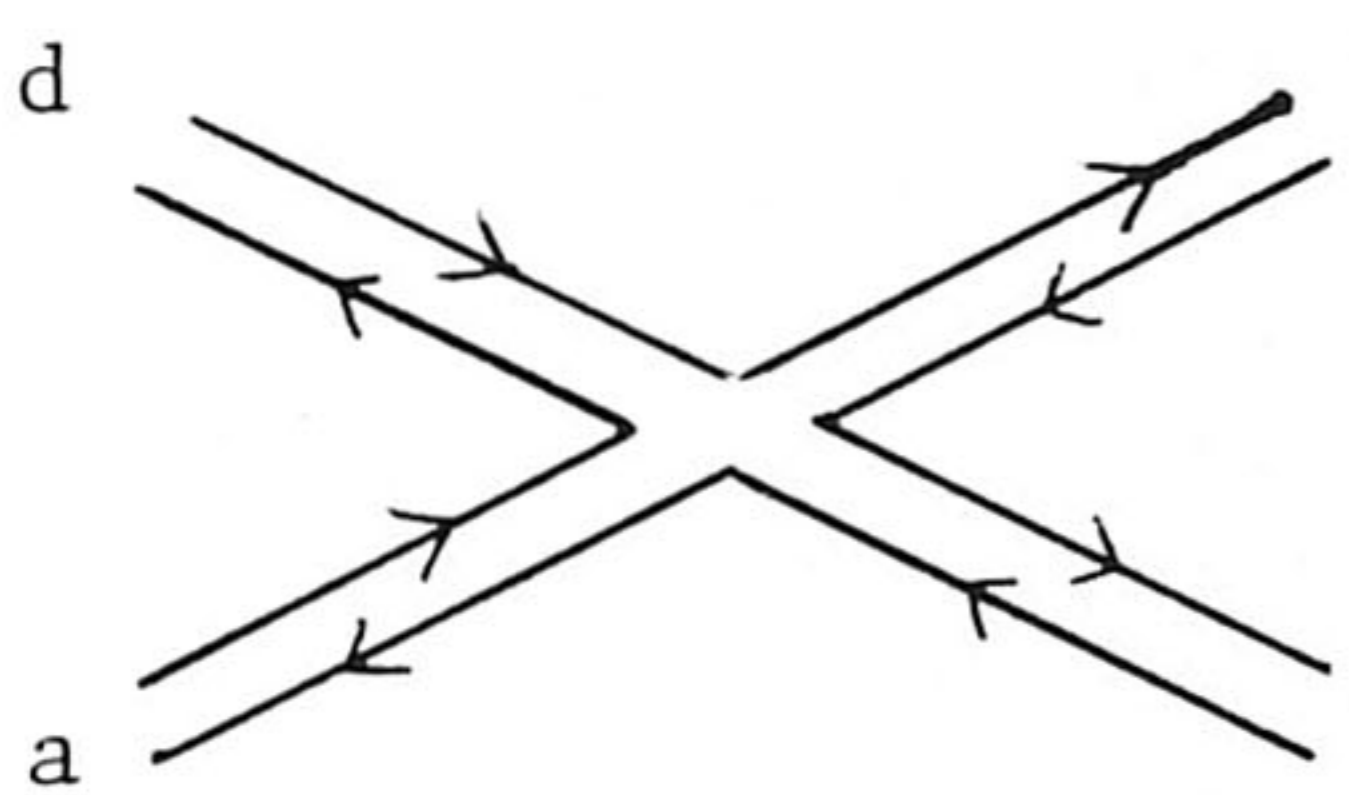
$$-g\, M_1^{bac}$$

$$-g^2\, M_2^{ba\ cd}$$

$$-g\, R_1^{\{abc\}}$$

$$-g^2\, R_2^{\{abcd\}}$$

Fig. 1: Feynman Rules at arbitrary N. The accolades { } stand for cyclic symmetrization with respect to the indices a,b,...

In that case an extra projection operator is required in the propagator:

$$\delta_i{}^k \delta_\ell{}^j - \frac{1}{N} \delta_i{}^j \delta_\ell{}^k \ . \tag{2.4}$$

The second term in (2.4) corresponds to an extra piece in the propagator, as given in Fig. 2. We will see later that such terms are relatively unimportant as $N \to \infty$.

For defining amplitudes it is often useful to consider source terms that preserve the (global) symmetry:

$$\mathcal{L}^{source} = J_\psi^{ab}(x)\psi^{*a}(x)\psi^b(x) + \tfrac{1}{2}J_A^{ab}(x) \operatorname{Tr} A^a(x)A^b(x) \ . \tag{2.5}$$

The corresponding notation in Feynman graphs is shown in Fig. 3.

3. THE $N \to \infty$ LIMIT AND PLANARITY

As usual, amplitudes and Green's functions are obtained by adding all possible (planar and non-planar) diagrams with their appropriate combinatorial factors. Note that, apart from the optional correction term in (2.4), the number N does not occur in Fig. 1. But, of course, the number N will enter into expressions for the amplitudes, and that is when an index-line closes. Such an index-loop gives rise to a factor

$$\sum_i \delta_i{}^i = N \ . \tag{3.1}$$

We are now in a position that we can classify the diagrams (with only gauge invariant sources as given by eq. (2.5)) according to their order in g and in N. Let there be given a connected diagram. First we consider the two-dimensional structure obtained by considering all closed index loops as the edges of little (simply connected) surface elements. All N x N matrix-propagators connect these surface elements into a bigger surface, whereas the N-vector-propagators form a natural boundary to the total surface. In the complex case the total surface is an oriented one; in the real case there is no orientation. In both cases the total surface may be multiply connected, containing "worm holes". For convenience we limit ourselves to the complex (oriented) case, and we close the surface by attaching extra surface elements to all N-vector-loops.

Let that surface have F faces (surface elements), P lines (propagators) and V vertices. We have $F = L + I + P_t$, where L is the number of N-vector-loops*) and I the number of index-loops; and we write (footnote: see next page)
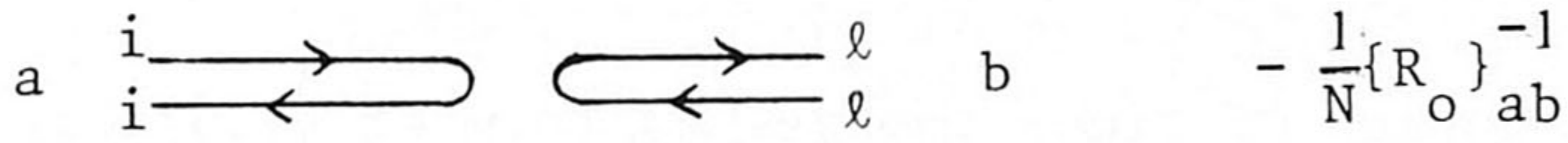
Fig. 2: Extra term in the propagator if Tr A is to be projected out.

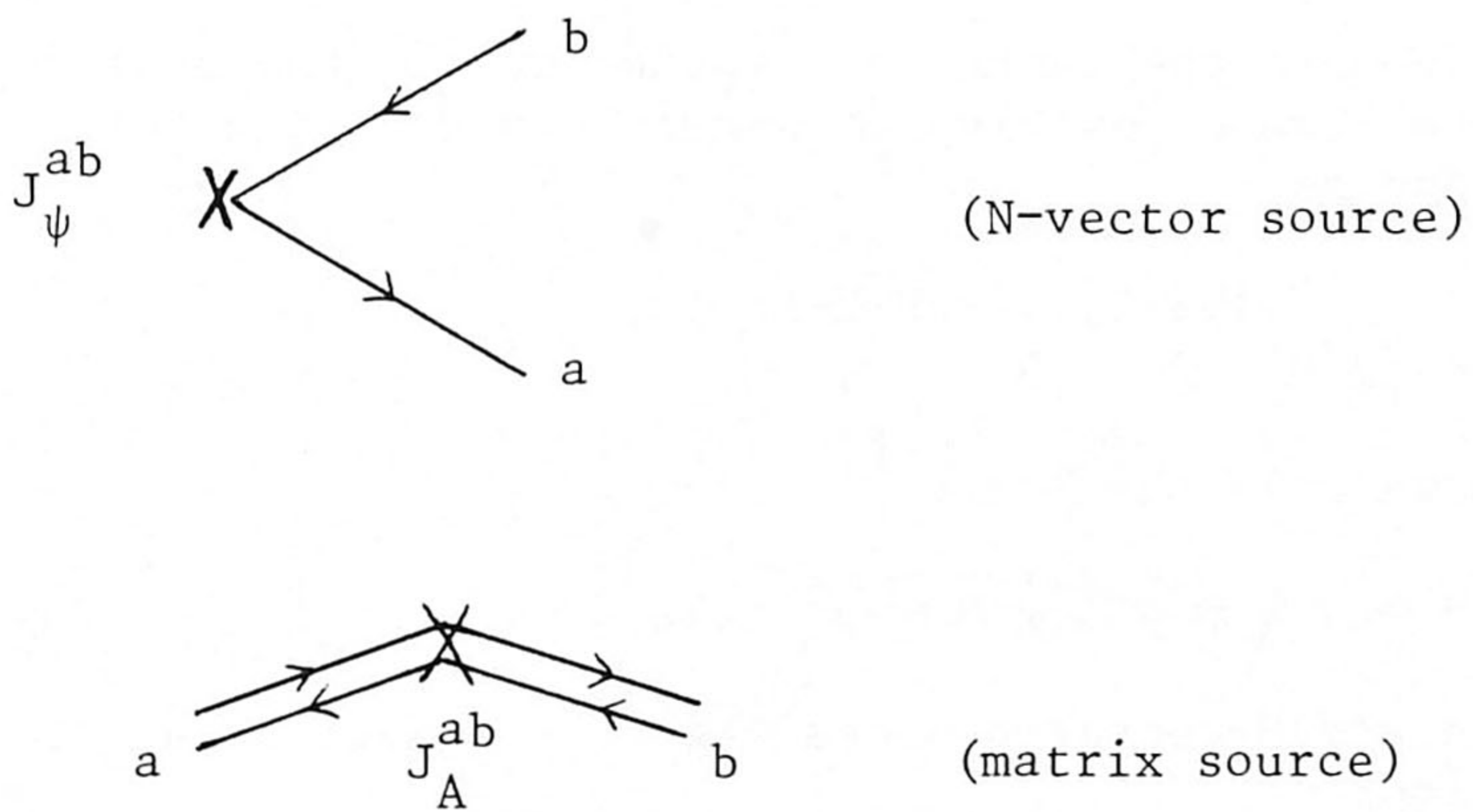$$-\frac{1}{N}\{R_o\}^{-1}_{ab}$$

Fig. 3: Invariant source insertions.

$$V = \sum_n V_n \, ,$$

where V_n is the number of n-point vertices. (V_2 is the number of source insertions). The diagram is now associated with a factor

$$r = g^{V_3 + 2V_4} \; N^{I - P_t} \, . \tag{3.2}$$

Here P_t is the number of times the second term of (2.4) has been inserted to obtain traceless propagators. By drawing a dot at each end of each propagator we find that the total number of dots is

$$2P = \sum_n n V_n \, , \tag{3.3}$$

and eq. (3.2) can be written as

$$r = g^{2P - 2V} \; N^{F - L - 2P_t} \, . \tag{3.4}$$

Now we apply a well-known theorem of Euler:

$$F - P + V = 2 - 2H \, , \tag{3.5}$$

where H counts the number of "wormholes" in the surface and is therefore always positive (a sphere has $H = o$, a torus $H = 1$, etc.). And so,

$$r = (g^2 N)^{\frac{1}{2}V_3 + V_4} \; N^{2 - 2H - L - 2P_t} \, . \tag{3.6}$$

Suppose we take the limit

$$N \to \infty \, , \; g \to o \, , \; g^2 N = \tilde{g}^2 \; \text{(fixed)} \, . \tag{3.7}$$

If there are N-vector-sources then there must be at least one N-vector-loop:

$$L \geqslant 1 \, .$$

The leading diagrams in this limit have $H = o$, $P_t = o$ and $L = 1$. They have one overall multiplicative factor N, and they are all planar: an open plane with the N-vector line at its edge (Fig. 4a).

---

*) "N-vector" here stands for N-component vector in U(N) space, so the N-vector-loops are the quark loops in quantum-chromo-dynamics.
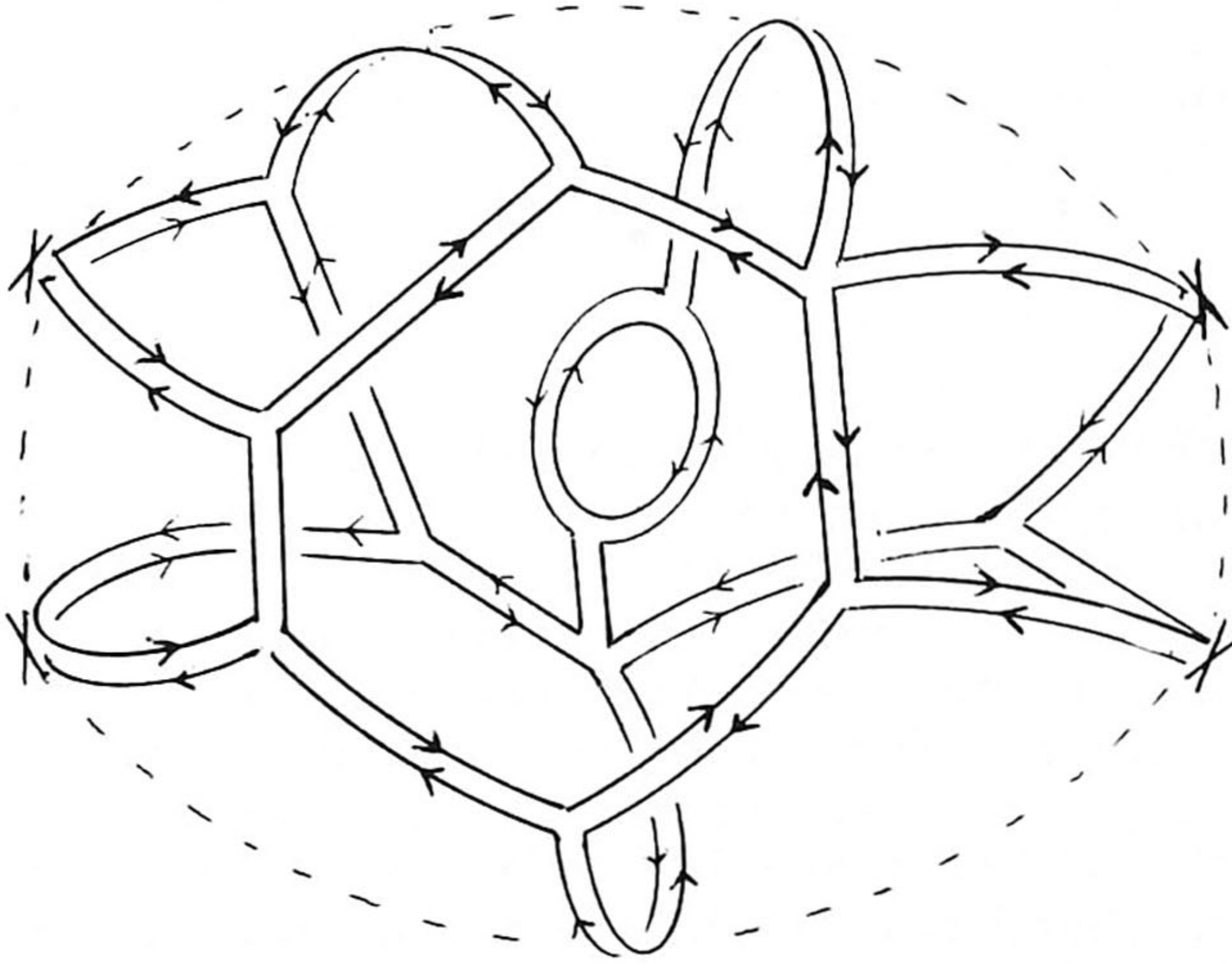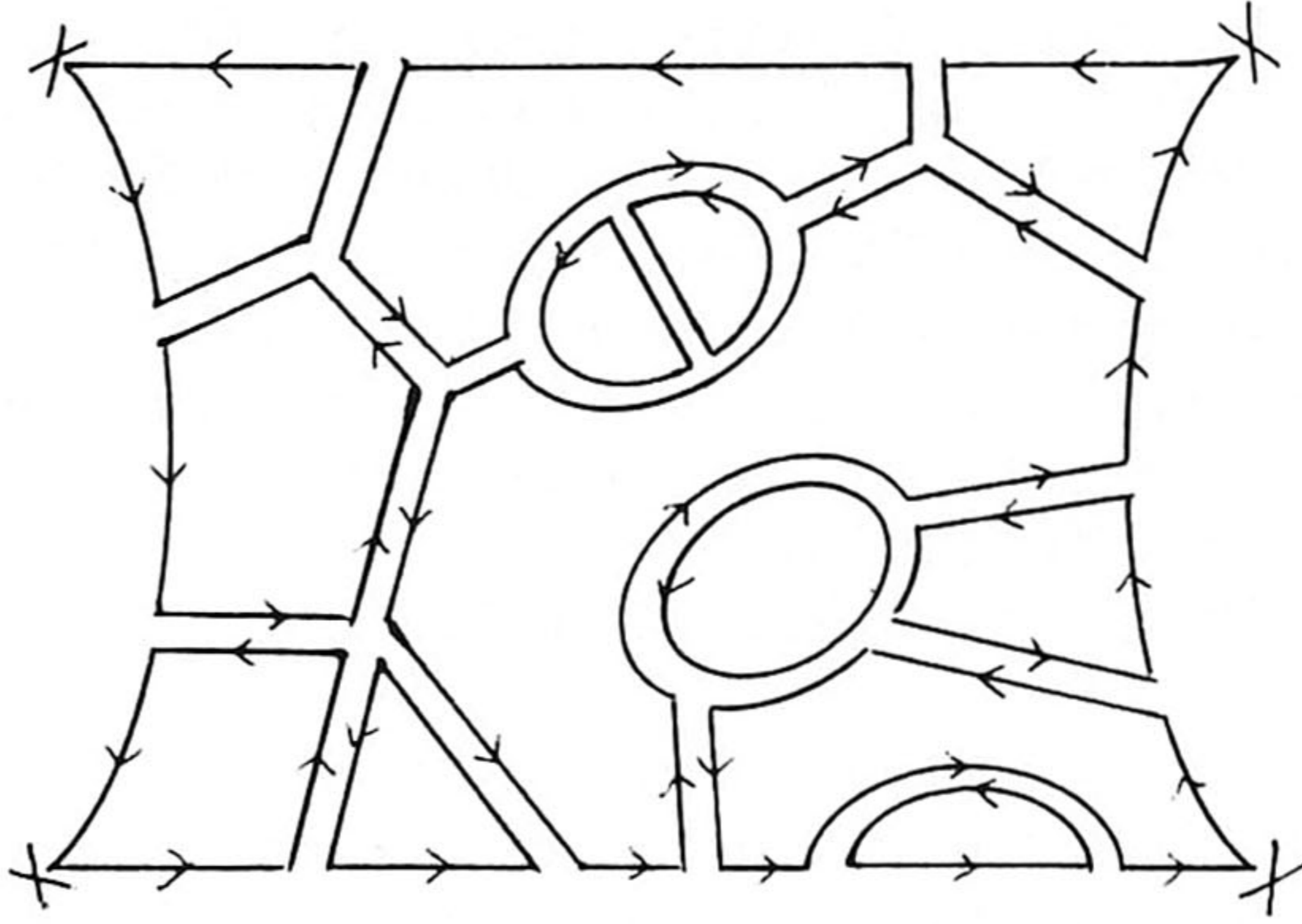
Fig. 4: Elements of the class of leading diagrams in the N → ∞
limit. a) If vector sources are present. b) In the absence
of vector sources (e.g. pure gauge theory).

If there are only matrix sources then $L \geq 0$. The leading diagrams all have the topology of a sphere and carry an overall factor N^2 (see Fig. 4b). We read off from eq. (3.6) that next to leading graphs are down by a factor $1/N$ for each additional N-vector-loop (= quark loop in quantum chromodynamics) and a factor $1/N^2$ for each "wormhole". Also the difference between U(N) and SU(N) theories disappears as $1/N^2$. It will be clear that this result depends only on the field variables being N-vectors and N x N matrices and the Lagrangian containing only single inner products or traces (not the *products* of inner products and/or traces). Diagrams with $L = 1$ and $H = 0$ are the easiest to visualize. In the sequel we discuss convergence aspects of the summation of those diagrams in all orders of $\tilde{g}$. Our main examples are

1) U(N) (or SU(N)) gauge theories with fermions in the N representation;

2) purely Lorentz scalar fields, both in N and in N x N representations of U(N). That theory will be called $Tr\lambda\phi^4$, or $-Tr\lambda\phi^4$, if λ is given the unusual sign. Both SU(N) gauge theory and $-Tr\lambda\phi^4$ are asymptotically free[9]. The latter has the advantage that one may add a mass term, so that it is also infrared convergent. However the fact that λ has the wrong sign implies that that theory only exists in the $N \to \infty$ limit, not for finite N. A model that combines all "good" features of the previous model is:

3) an SU(N) Higgs theory with N Higgs fields in the elementary representation, N fermions in the elementary representation and a fermion in the adjoint representation. A global SU(N) symmetry then survives. All vector, spinor and scalar particles are massive, and it is asymptotically free if $\tilde{h}^2/\tilde{g}^2 = 1$;

$$\tilde{\lambda}/\tilde{g}^2 = \frac{1}{8}(\sqrt{129}-5) , \qquad (3.8)$$

where h is a Yukawa coupling constant and λ the Higgs self coupling. The reason for mentioning this model is that it is asymptotically free in the ultraviolet, and it is convergent in the infrared, so that our methods will enable us to construct it rigorously in the $N \to \infty$ limit (provided that masses are chosen sufficiently large and the coupling constant sufficiently small), and positivity of the Hamiltonian is guaranteed also for finite N so that there is every reason for hope that the theory makes sense also at finite N, contrary to the $-\lambda Tr\phi^4$ theory. This model is described in appendix A.

4. THE SKELETON EXPANSION

From now on we consider diagrams of the type pictured in figure 4a ($H = 0$, $L = 1$). They all have the same N dependence, so once we restricted ourselves to these planar diagrams only we may drop the indices i,j,... and replace the double-line propagators by single lines. Often we will forget the tilde (~) on g^2 because

the factor N is always understood. Only the (few) indices a,b,...
of eq. (2.1), as far as they do not refer to the SU(N) group(s),
are kept. The details of this surviving index structure are not
important for what follows, as long as the Feynman rules (Fig. 1)
are of the general renormalizable type.

Our first concern will be the isolation of the ultraviolet
divergent parts of the diagrams. For this we use an ancient
device[10] called "skeleton-expansion" *). It can be applied to any
graph, planar or not, but for the planar case it is particularly
useful.

Consider a graph with at least five external lines. A one-
particle irreducible subgraph is a subset of more than one
vertices with the internal lines that connect these vertices, that
is such that if one of the internal lines is cut through then the
subgraph still remains connected. We now draw boxes around all
one-particle irreducible subgraphs that have four of fewer ex-
ternal lines. In general one may get boxes that are partially
overlapping. A box is *maximal* if it is not entirely contained
inside a larger box.

Theorem: All maximal boxes are not-overlapping. This means that
two different maximal boxes have no vertex in common.

Proof: If two maximal boxes A and B would overlap then at least
one vertex x_1 would be both in A and B. There must be a vertex x_2
in A but not in B, otherwise A would not be maximal. Similarly
there is an x_3 in B but not in A. Now A was irreducible, so that
at least two lines connect x_1 with x_2. These are external lines of
B but not of A U B. Now B may not have more than 4 external lines.
So not more than two external lines of A U B are also external
lines of B. The others may be external lines of A. But there can
also be not more than two of those. So A U B has not more than
four external lines and is also irreducible since A and B are, and
they have a vertex in common. So we should draw a box around A U B.
But then neither A nor B would be maximal, contrary to our
assumption. No planarity was needed in this proof.

The skeleton graph of the diagram is now defined by replacing
all maximal boxes by single "dressed" vertices. Any diagram can
now be decomposed into its "skeleton" and the "meat", which is the
collection of all vertex and self-energy insertions at every two-,
three- and four-leg irreducible subgraph. In particular the self-

---

*) The method described here differs from Bjorken and Drell[10] in
   that we do not distinguish fermions from bosons, so that also
   subgraphs with four external lines are contracted.

energy insertions build up the so-called dressed propagator. We call the dressed three- and four-vertices and propagators the "basic Green functions" of the theory. They contain all ultra-violet divergences of the theory. The rest of the diagram, the "skeleton" built out of these basic Green functions is entirely void of ultraviolet divergencies because there are no further (sub)graphs with four of fewer external lines, which could be divergent.

The skeleton expansion is an important tool that will enable us to construct in a rigorous way the planar field theory. For, under fairly mild assumptions concerning the behavior of the basic Green functions we are able to prove that, given these basic Green functions, the sum of all skeleton graphs contributing to a certain amplitude *in Euclidean space* is absolutely convergent (not only Borel summable). This proof is produced in the next 6 sections. Clearly, this leaves us to construct the basic Green functions themselves. A recursive procedure for doing just that will be given in sects. 12-15. Indeed we will see that our original assumptions concerning these Green functions can be verified provided the masses are big and the coupling constants small, with one exception: in the scalar $-\lambda \mathrm{Tr}\phi^4$ theory the skeleton expansion always converges even if the bare (minimally subtracted) mass vanishes! (sect. 18)

5. TYPE IV PLANAR FEYNMAN RULES

We wish to prove the theorem mentioned in the previous section: given certain bounds for the basic Green functions, then the sum of all skeleton graphs containing these basic Green functions inside their "boxes" converges in the absolute. In fact we want a little more than that. In sects. 13-15 we will also require bounds on the total sum. Those in turn will give us the basic Green functions. We have to anticipate what bounds those will satisfy. In general one will find that the basic Green functions will behave much like the bare propagators and vertices, with deviations that are not worse than small powers of ratios of the various momenta. Note that all our amplitudes are *Euclidean*.

First we must know how the dressed propagators behave at high and low momenta. The following bounds are required:

$$|P_{ab}(k)| \geqslant \frac{Z(k)}{k^2+m^2} \ , \qquad \text{if } k^2 \geqslant o \ . \tag{5.1}$$

Here $P_{ab}(k)$ is the propagator. From now on we use the absolute value symbol for momenta to mean: $|p| = \sqrt{p^2+m^2}$. Then the field renormalization factor $Z(k)$ is approximately:

$$Z(k) \cong \left[\log\left(1 + \frac{|k|}{m} \right) \right]^{\sigma} , \tag{5.2}$$

where σ is a coefficient that can be computed from perturbation expansion. The mass term in (5.1) is not crucial for our procedure but m in (5.2) can of course not be removed easily.

To write down the bounds on the three- and four-point Green functions in Euclidean space we introduce a convenient notation to indicate which external momenta are large and which are small.

For any planar Green function we label not the external momenta but the spaces in between two external lines by indices 1,2,3,... which have a cyclic ordering. An external line has momentum

$$p_{i,i+1} \overset{=}{\text{def}} p_i - p_{i+1} . \tag{5.3}$$

We have automatically momentum conservation,

$$\sum_i p_{i,i+1} = o , \tag{5.4}$$

and the p_i are defined up to an overall translation,

$$p_i \rightarrow p_i + q , \quad \text{all } i . \tag{5.5}$$

A channel (any in which possibly a resonance can occur) is given by a pair of indices, and the momentum through the channel is given by

$$p_{i,j} = p_i - p_j . \tag{5.6}$$

So we can look at the p_i as dots in Euclidean momentum space, and the distance between any pair of dots is the momentum through some channel. If we write

$$(((12)_{A_1} \, 3)_{A_2} \, 4)_{A_3} , \tag{5.7}$$

or simply $(((12)_1 \, 3)_2 \, 4)_3$, then this means:

$$|p_1 - p_2| = A_1 \quad ,$$

$$|p_1 - p_3| = A_2 \gg A_1 ,$$

$$|p_1 - p_4| = A_3 \gg A_2 . \tag{5.8}$$

So the brackets are around momenta that form close clusters.

Our bounds for the three- and four-point functions are now defined in table 1.

Table 1

Bounds for the 3- and 4-point dressed Green functions. Z_{ij} stands for $Z(p_i-p_j)$. All other exceptional momentum configurations can be obtained by cyclic rotations and reflections of these. K_i are coefficients close to one.
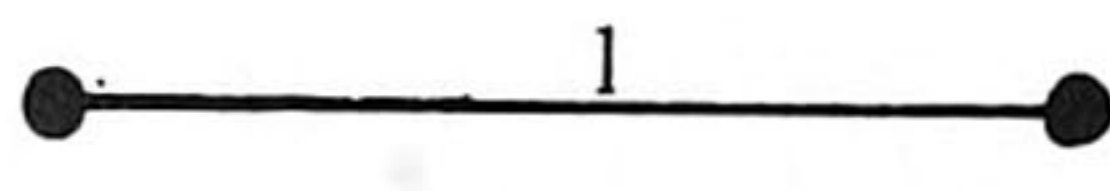
$((12)_1\ 3)_2$	$K_1(Z_{12}Z_{23}Z_{31})^{-\frac{1}{2}} A_2(A_2/A_1)^\alpha\, g(A_2)$
$(((12)_1\ 3)_2\ 4)_3$	$K_2^2(Z_{12}Z_{23}Z_{34}Z_{41})^{-\frac{1}{2}}\ (A_2/A_1)^\alpha\ (A_3/A_2)^\beta\ g^2(A_3)$
$((12)_1\ (34)_2)_3$	$K_3^2(Z_{12}Z_{23}Z_{34}Z_{41})^{-\frac{1}{2}}\ (A_3^2/A_1A_2)^\alpha\ g^2(A_3)$
$(((13)_1\ 2)_2\ 4)_3$	$K_4^2(Z_{12}Z_{23}Z_{34}Z_{41})^{-\frac{1}{2}}\ (A_2A_3/A_1^2)^\beta\ g^2(A_3)$
$((13)_1\ (24)_2)_3$	$K_5^2(Z_{12}Z_{23}Z_{34}Z_{41})^{-\frac{1}{2}}\ (A_3/A_1)^{2\beta}\ g^2(A_3)$
	if $A_1 \leqslant A_2$
$((123)_1\ 4)_2$	$K_6^2(Z_{12}Z_{23}Z_{34}Z_{41})^{-\frac{1}{2}}\ (A_2/A_1)^\beta\ g^2(A_2)$
$((12)_1\ 34)_2$	$K_7^2(Z_{12}Z_{23}Z_{34}Z_{41})^{-\frac{1}{2}}\ (A_2/A_1)^\alpha\ g^2(A_2)$

Here α and β are small positive coefficients. $g(x)$ is a slowly varying running coupling constant. For the time being all we need is some g with
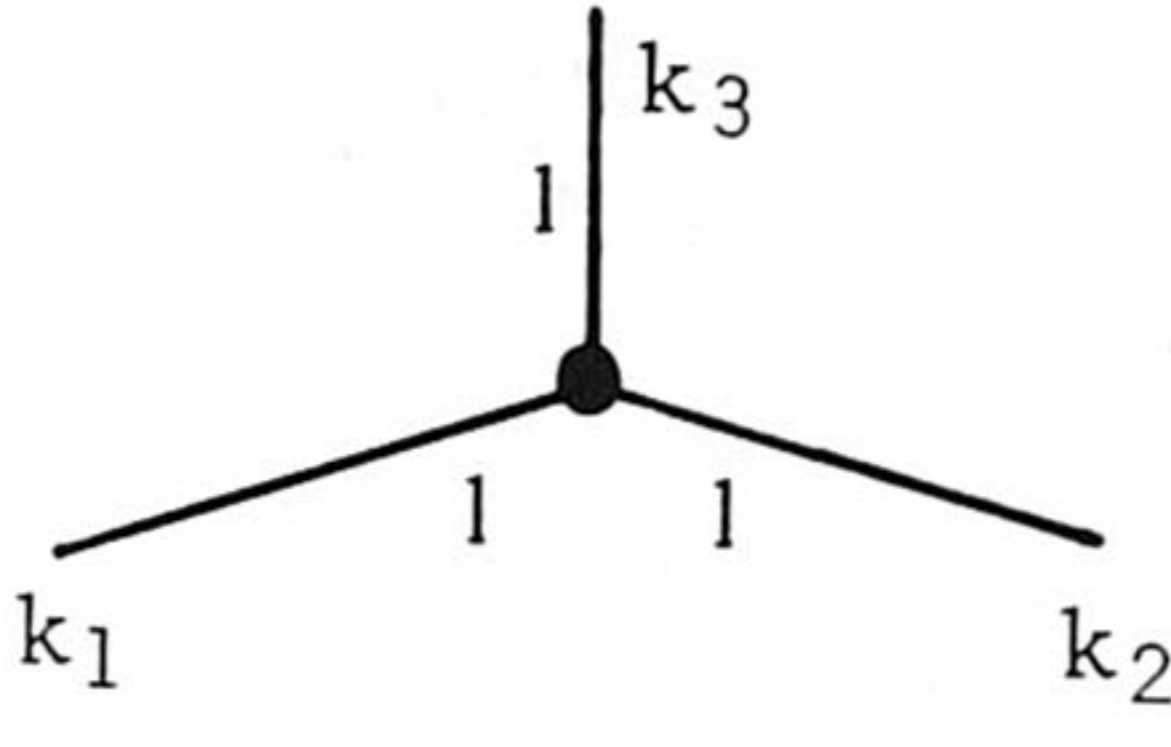
$$\max_i K_i\, g(x) \leqslant g \qquad \text{for all } x\ , \tag{5.9}$$

where we also assume that possible summation over indices a,b,... is included in the K coefficients. Clearly the bare vertices would satisfy the bounds with $\alpha = \beta = 0$. Having positive α and β allows us to have any of the typical logarithmic expressions coming from the radiative corrections in these dressed Green functions. Indeed we will see later (sect. 13) that those logarithms will never surpass our power-laws.
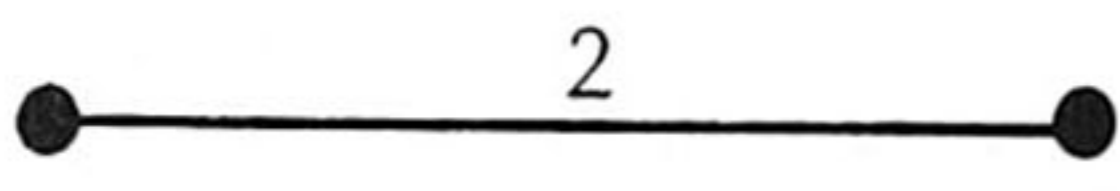
Table 1 has been carefully designed such that it can be re-obtained in constructing the basic Green functions as we will see in sects. 12-14. First we notice that the field renormalization factors $Z(p_i-p_j)^{-\frac{1}{2}}$ cancel against corresponding factors in our bounds for the propagator (5.1). The power-laws of Table 1 can be conveniently expressed in terms of a revised set of Feynman rules. These are given in Fig. 5. We call them type IV Feynman rules after a fourth attempt to reformulate our bounds (types I, II and
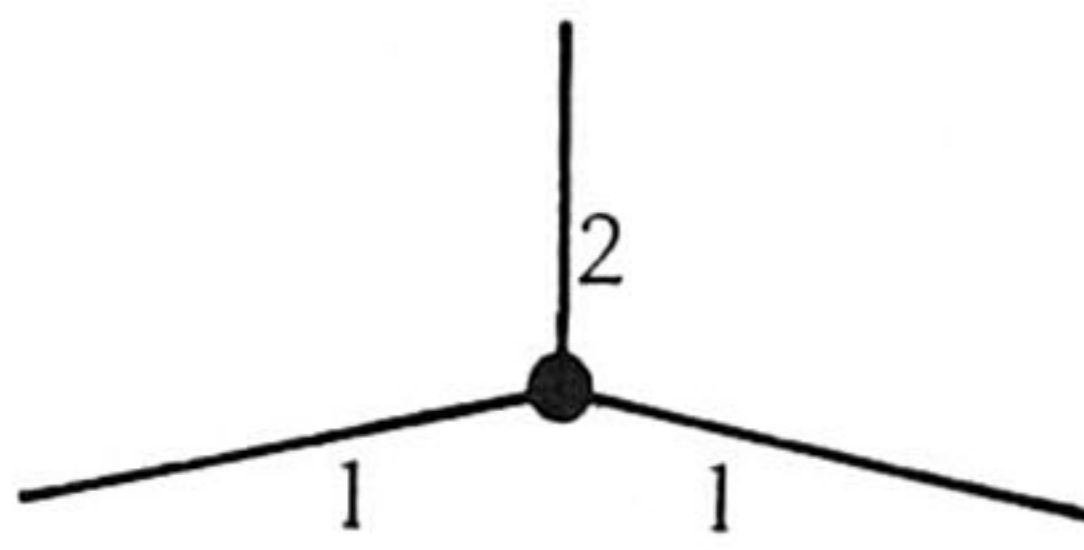
$$\frac{1}{(k^2+m^2)^{1+\alpha}}$$ (dressed elementary propagator)

$$g[\max(|k_1|,|k_2|,|k_3|)]^{1+3\alpha}$$ (dressed 3-vertex)

$$\frac{1}{|k|^{2\beta}}$$ (composite propagator)

$$g[\max(|k_1|,|k_2|,|k_3|)]^{2\alpha+\beta}$$

$$g[\max(|k_1|,|k_2|,|k_3|)]^{\alpha+2\beta-1}$$ (generalized vertices)

$$g[\max(|k_1|,|k_2|,|k_3|)]^{3\beta-2}$$

$$|k|^{-\alpha}$$ (external line)

Fig. 5: Type IV Feynman Rules. $|k|$ stands for $\sqrt{k^2+m^2}$.

III occur in refs. 11, 12 and are not needed here). The trick is
to introduce a new kind of propagator, •——2——• , that represents
an exchange of two or more of the original particles in the dia-
gram we started off with.

The procedure adapted in these lectures deviates from earlier
work[11] in particular by the introduction of the last two vertices
in Fig. 5. Notice that they decrease whenever two of the three ex-
ternal momenta become large.

It is now a simple exercise to check that indeed any diagram
built from basic Green functions that satisfy the bounds of Table
1 can also be bounded by corresponding diagram(s) built from type
IV Feynman rules. The four-vertex is simply considered as a sum of
two contributions both made by connecting two three-point vertices
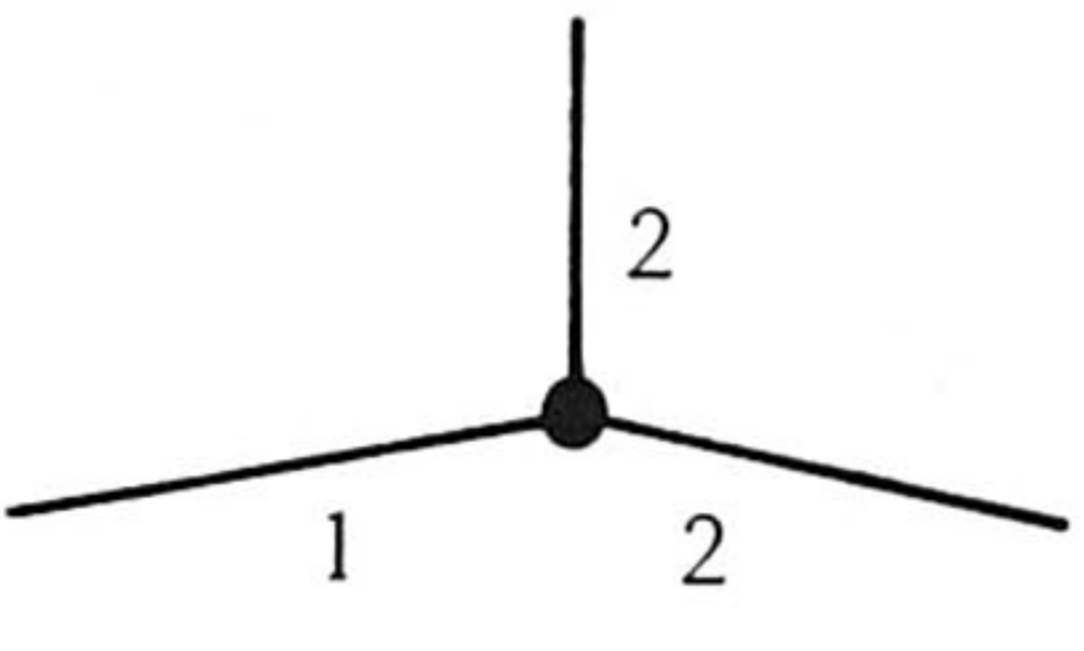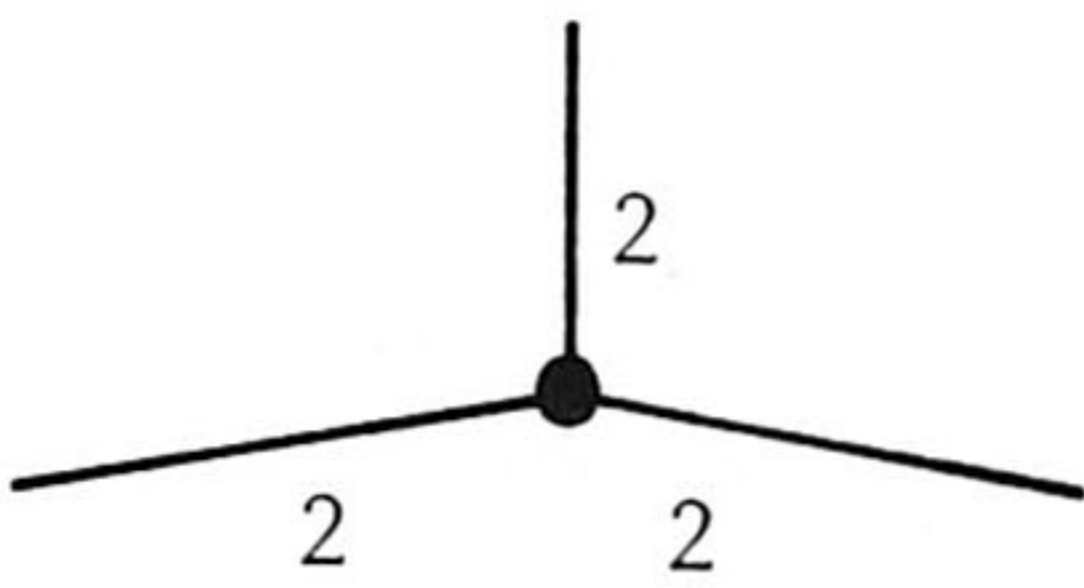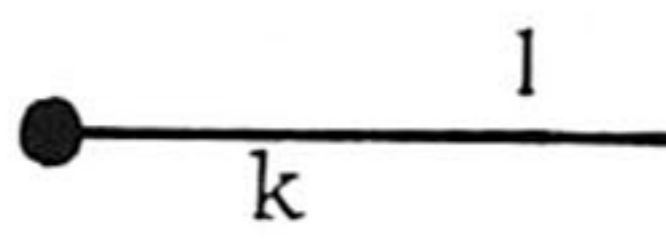with a composite propagator, and the factors $|k|^{-\alpha}$ from the propa-
gators in Fig. 5 are considered parts of the vertex functions (the
mass term of the propagator may be left out; it is needed at a
later stage).

Elementary power counting now tells us that the superficial
degree of convergence, Z, of any (sub)graph with E_1 external
single lines and E_2 external composite lines is given by

$$Z = (1-\alpha)E_1 + (2-\beta)E_2 - 4 . \qquad (5.10)$$

Since we consider only skeleton graphs, all our graphs and sub-
graphs have

$$E_1 + 2E_2 \geqslant 5 . \qquad (5.11)$$

Thus, Z is guaranteed to be positive if we restrict our coef-
ficients by

$$o < \alpha < 1/5 ;$$

$$o < \beta < 2/5 . \qquad (5.12)$$

(Infrared convergence would merely require $\alpha < 1$; $\beta < 2$, and is
therefore guaranteed also.) So we know that with (5.12) all graphs
and subgraphs are ultraviolet and infrared convergent. The theorem
we now wish to prove is: the sum of all convergent type IV dia-
grams contributing to any given amplitude with 5 (or more) ex-
ternal lines converges in Euclidean space. It is bounded by the
sum of all type IV tree graphs (graphs without closed loops)
multiplied with a fixed finite coefficient.

A further restriction on the coefficients α and β will be
necessary (eq. (8.15)).

6. NUMBER OF TYPE IV DIAGRAMS

The total number $G(E,L)$ of connected or irreducible planar diagrams with E external lines and L closed loops in any finite set of Feynman rules, is bounded by a power law (in contrast with the non-planar diagrams that contribute for instance to the Lth order term in the expansion such as (1.1) for a simple functional integral):

$$G(E,L) \leqslant C_1^E C_2^L , \qquad (6.1)$$

for some C_1 and C_2.

In some cases C_1 and C_2 can be computed exactly and even closed expressions for $G(E,L)$ exist[8]. These mathematical exercises are beautiful but rather complicated and give us much more than we really need. In order to make these lectures reasonably self-sustained we will here derive a crude but simple derivation of ineq. (6.1) yielding C coefficients that can be much improved on, with a little more effort.

Let us ignore the distinction between the two types of propagators and just count the total number $G(E,L)$ of connected planar ϕ^3 diagrams with a given configuration of E external lines and L closed loops. We have (see Fig. 6)

$$G(E+1,L) = G(E+2,L-1) + \sum_{n,L_1} G(n+1,L_1)G(E+1-n,L-L_1) . \qquad (6.2)$$

$$G(E,L) \quad = o \quad if \quad E < 2 \quad or \ if \quad L < o ;$$

$$G(2,o) \quad = 1 . \qquad (6.3)$$
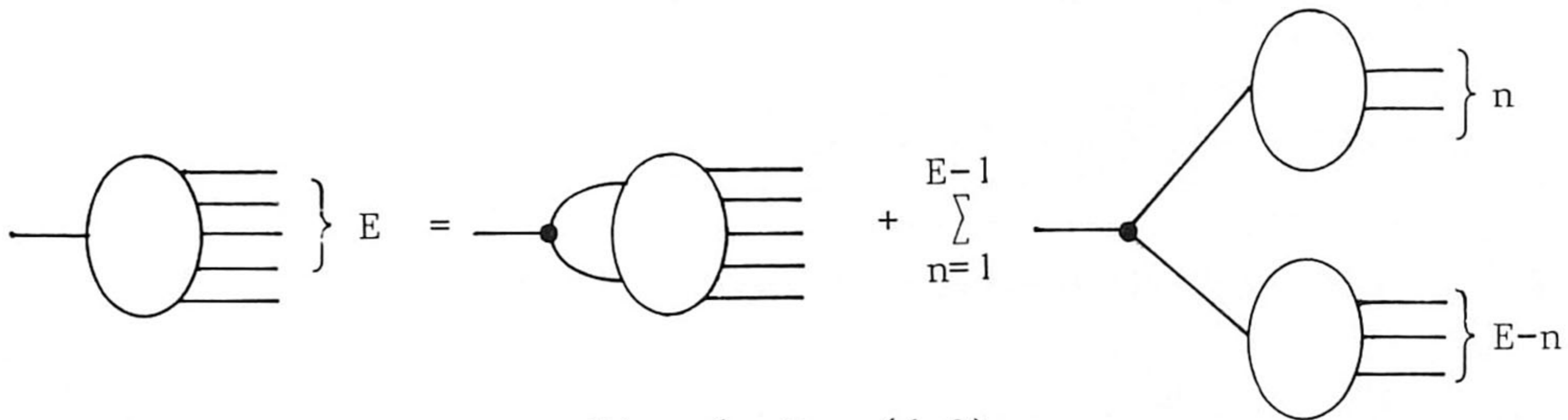
Fig. 6: Eq. (6.2)

We wish to solve, or at least find bounds for, $G(E,L)$ from (6.2) with boundary condition (6.3). A good guess is to try

$$G(E,L) \leqslant \frac{C_0 C_1^E C_2^L}{(E-1)^2 (L+1)^2} \ , \ E \geqslant 2 \ , \ L \geqslant o \ , \tag{6.4}$$

which is compatible with (6.3) if

$$C_0 C_1^2 \geqslant 1 \ . \tag{6.5}$$

Using the inequality

$$\sum_{n=1}^{k} \frac{1}{n^2 (k-n)^2} \leqslant \frac{4}{k^2} \ , \tag{6.6}$$

we find that the r.h.s. of (6.2) will be bounded by

$$\frac{C_0 C_1^{E+2} C_2^{L-1}}{(E+1)^2 L^2} + \frac{16 C_0^2 C_1^{E+2} C_2^L}{(E-1)^2 (L+1)^2} \ , \tag{6.7}$$

which is smaller than

$$\frac{C_0 C_1^{E+1} C_2^L}{E^2 (L+1)^2} \ , \tag{6.8}$$

if

$$4C_1/C_2 + 64 C_0 C_1 \leqslant 1 \ . \tag{6.9}$$

This is not incompatible with (6.5) although the best "solution" to these two inequalities is an uncomfortably large set of values for C_0, C_1 and C_2. But we proved that they are finite.

The exact solution to eq. (6.2) is

$$G(E,L) = \frac{2^L (2E-2)! (2E+3L-4)!}{L! (E-1)! (E-2)! (2E+2L-2)!} \ , \tag{6.10}$$

which we will not derive here. Using

$$\frac{(A+B)!}{A! B!} \leqslant 2^{A+B-1} \tag{6.11}$$

we find that in (6.1),

$$C_1 \leqslant 16 \ ; \ C_2 \leqslant 16 \ . \tag{6.12}$$

For fixed E, in the limit of large L,

$$C_2 \rightarrow 27/2 \ . \tag{6.13}$$

Similar expressions can be found for the set of irreducible diagrams. Since they are a subset of the connected diagrams we expect C coefficients equal to or smaller than the ones of eqs. (6.12) and (6.13). Limiting oneself to only convergent skeleton graphs will reduce these coefficients even further.

We have for the number of vertices V

$$V = E + 2L - 2 \ , \tag{6.14}$$

and the number of propagators P:

$$P = V + L - 1 \ . \tag{6.15}$$

So, if different kinds of vertices and propagators are counted separately then the number of diagrams is multiplied with

$$C_V^V C_P^P \ , \tag{6.16}$$

which does not alter our result qualitatively. Also if there are elementary 4-vertices then these can be considered as pairs of 3-vertices connected by a new kind of propagators, as we in fact did. So also in that case the numbers of diagrams are bounded by expressions in the form of eq. (6.1).

7. THE SMALLEST FACETS

We now wish to show that every planar type IV diagram with L loops is bounded by a coefficient C^L times a (set of) type IV tree graph(s), with the same momentum values at the E external lines. This will be done by complete induction. We will choose a closed loop somewhere in the diagram and bound it by a tree insertion. Now even in a planar diagram some closed loops can become quite large (i.e. have many vertices) and it will not be easy to write down general bounds for those. Can we always find a "small" loop somewhere?

We call the elementary loops of a planar diagram facets. Now Euler's theorem for planar graphs is:

$$V - P + L = 1 \ . \tag{7.1}$$

Take an irriducible diagram. Write

$$L = \sum_n F_n \, , \tag{7.2}$$

where F_n are the number of facets with exactly n vertices (or "corners"). Let

$$P = P_i + P_e \, , \tag{7.3}$$

where P_i is the number of internal propagators and P_e is the number of propagators at the edges of the diagram. Then, by putting a dot at every edge of each facet and counting the number of dots we get

$$\sum_n n F_n = 2P_i + P_e \, . \tag{7.4}$$

For the numbers V_n of n-point vertices we have similarly

$$\sum_n n V_n = 2P + E \, , \tag{7.5}$$

but in ourcase we only consider 3-point vertices (compare eqs. (6.14) and (6.15)):

$$3V = 2P + E \, . \tag{7.6}$$

Combining eqs. (7.1) - (7.6) we find

$$\sum_n (n-6) F_n = 2E - P_e - 6 \, . \tag{7.7}$$

This equation tells us that if a diagram has

$$L \geqslant 2E - 8 \tag{7.8}$$

then either it is a "seagull graph" ($P_e \leqslant 1$) which we usually are not interested in, or there must be at least one subloop with 6 or fewer external lines:

$$F_n > 0 \quad \text{for some} \quad n \leqslant 6 \, . \tag{7.9}$$

So diagrams with given E and large enough L must always contain facets that are either hexagons or even smaller.

In fact we can go further:
theorem: if a planar graph (with only 3-vertices) and all its irreducible subgraphs have $2E - P_e \geqslant 6$ then the entire graph obeys

$$L \leqslant \frac{E^2}{12} - \frac{E}{2} + 1 \, . \tag{7.10}$$

This simple theorem together with eq. (7.7) tells us that any dia-
gram with a number of loops L exceeding the bound of (7.10) must
have at least one elementary facet with 5 of fewer lines attached
to it. Although we could do without it, it is a convenient theorem
and now we devote the rest of this section to its proof (it could
be skipped at first reading).

First we remark that if we have the theorem proven for all
irreducible graphs up to a certain order, then it must also hold
for reducible graphs up to the same order. This is because if we
connect two graphs with one line we get a graph 3 with

$$L_3 = L_1 + L_2 \ ,$$

$$P_{e3} = P_{e1} + P_{e2} + 2 \ , \tag{7.11}$$

$$E_3 = E_1 + E_2 - 2 \ .$$

If L_1, E_1 and L_2, E_2 satisfy (7.10) then so do L_3 and E_3 (remember
that E and L are integers and the smallest graph with L > o has E =
6; propagators that form two edges of a diagram are counted twice in P_e).

Forthe irreducible graphs we prove (7.10) by a rather unusual
induction procedure for planar graphs. We consider the outer rim
of an irreducible graph and all the (in general not irreducible)
graphs inside it (see Fig. 7). Let the entire graph have E ex-
ternal lines and P_e propagators at its sides. The subgraphs i
inside the rim have e_i external lines and P_{ei} propagators at their
sides. We count:

$$P_e = E + \sum_i e_i \ , \tag{7.12}$$

and the number of loops L of the entire diagram is

$$L = 1 + \sum_i (L_i + e_i - 1) \ . \tag{7.13}$$

Now each facet between the subgraphs and the rim must have at
least 6 propagators as supposed, therefore

$$P_e + \sum P_{ei} + 2 \sum e_i \geqslant 6 \sum_i (e_i - 1) + 6 \ , \tag{7.14}$$

but if some of the subgraphs are single propagators we need to be
more precise

$$P_e + \sum P_{ei} + 2 \sum e_i \geqslant 6 \sum_i (e_i - 1) + 6 + 2N_2 \ , \tag{7.15}$$
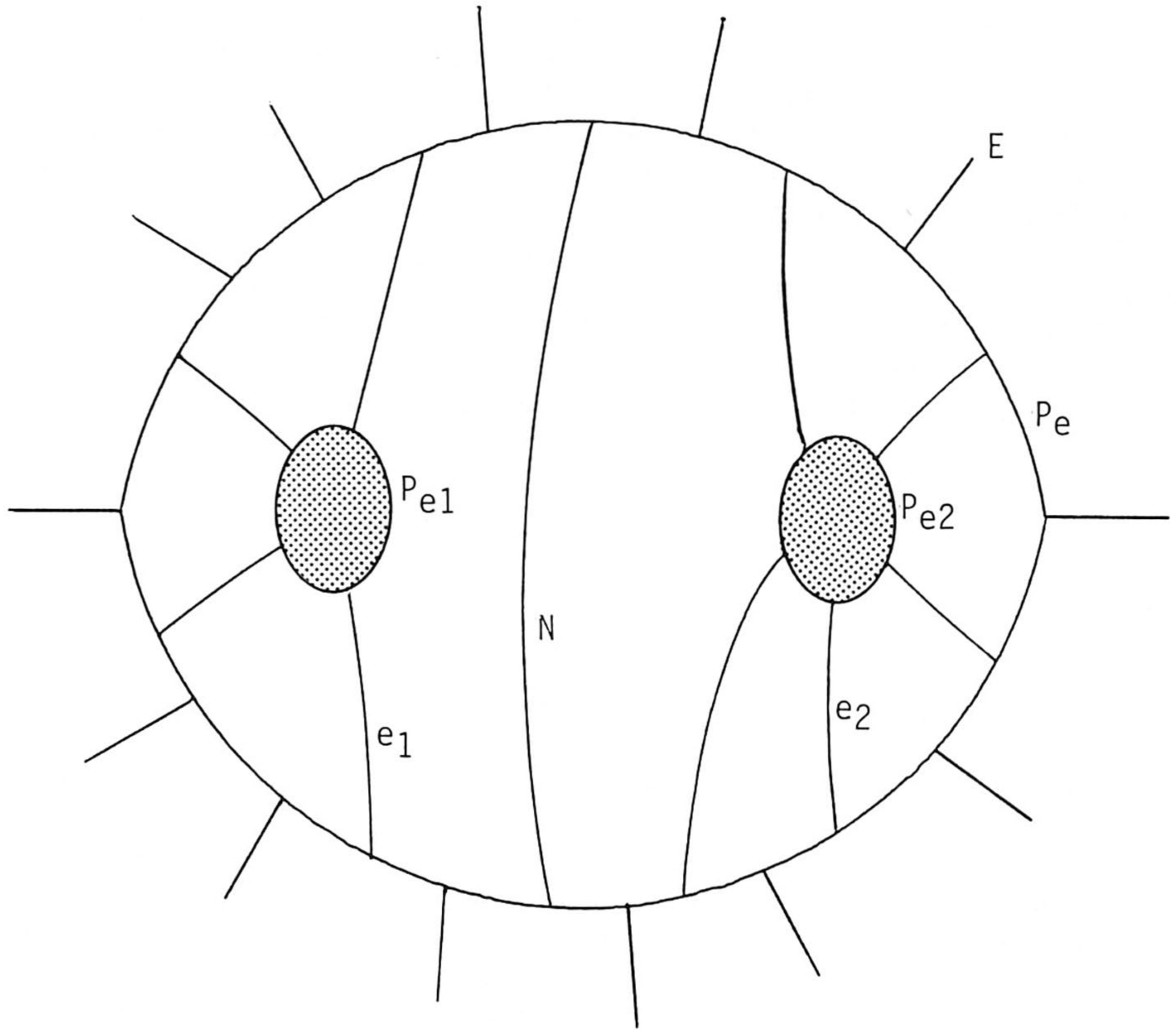
Fig. 7: Proving the theorem of sect. 7. The number E counts the
external lines of the entire graph. P_e the number of
sides and e_i and P_{ei} do the same for the subgraphs 1 and 2.
N is the number of single propagators.

where N_2 is the number of single propagators, each of which
contributes with $e = 2$ in eq. (7.13), and have $P_{ei} = o$. Now we use
(7.12), and

$$P_{ei} \leqslant 2e_i - 6 , \qquad\qquad (7.16)$$

as required, whereas $\Sigma(2e-6) + 2N_2 = o$ for the single propagators,
to arrive at

$$E \geqslant \sum_i e_i + 6 . \qquad\qquad (7.17)$$

From the assumption that all subraphs already satisfy (7.10) we
get, writing $L_1 = \sum_i L_i$ and $E_1 = \sum_i e_i$:

$$L_1 \leqslant \frac{E_1^2}{12} - \frac{E_1}{2} + 1 \; , \tag{7.18}$$

and from (7.13)

$$L \leqslant L_1 + E_1 \; . \tag{7.19}$$

With (7.17) which reads $E \geqslant E_1 + 6$ we now see that (7.10) again holds for the entire diagram. The quadratic expression in (7.10) is the sharpest that can be derived from (7.17)-(7.19), and indeed large diagrams that saturate the inequality can be found, by joining hexagons into circular patterns.

Our conclusion is that if we wish to use an induction procedure to express a bound for diagrams with type IV Feynman rules and L loops in terms of one with a smaller number L' loops we can try to do that by replacing successively triangles, qudrangles and/or pentagons by type IV tree insertions, until the bound (7.10) is reached. In particular if $E = 5$ this leads us to a tree diagram. The next three sections show how this procedure works in detail.

8. TRIANGLES

Consider a (large) diagram with type IV Feynman rules. We had already decreed that it and all its subgraphs are ultraviolet and infrared convergent (divergent subgraphs had been absorbed into the vertices and propagators before). With eqs. (5.10)-(5.12) this means that each subgraph has

$$E_1 + 2E_2 \geqslant 5 \; , \tag{8.1}$$

so, in particular, there are no self-energy blobs. First we use the inequality of Fig. 8 to replace composite propagators by ordinary dressed propagators one by one until ineq. (8.1) forbids any further such replacements. The inequality is readily proven: we write for the propagators with its vertices:·

Fig. 8. A composite propagator is smaller than an elementary one.

$$|p_1|^{1+\alpha_1+\alpha_2+\gamma} \, |p_2|^{1+\alpha_3+\alpha_4+\gamma} \, |k^2|^{-1-\gamma} \, , \qquad (8.2)$$

where k is the momentum through the propagator, $|p_1| \geqslant |k|$. $|p_2| \geqslant |k|$, and $\alpha_i = \alpha$ for a dressed propagator, and $\alpha_i = \beta-1$ for a composite propagator. At the left hand side $\gamma = \beta-1$, and at the right hand side $\gamma = \alpha$. Clearly we have

$$\left(\frac{|p_1||p_2|}{k^2}\right)^{\beta-1} \leqslant \left(\frac{|p_1||p_2|}{k^2}\right)^{\alpha} \, , \qquad (8.3)$$

α and β being both close to zero due to (5.12).

Now consider all elementary triangle loops in our diagram. Under what conditions can we replace them by type IV 3-vertices (Fig. 9)? Due to (8.1) there can be at most one elementary (dressed external line, the others are composite: $E_2 = 2$ or 3;
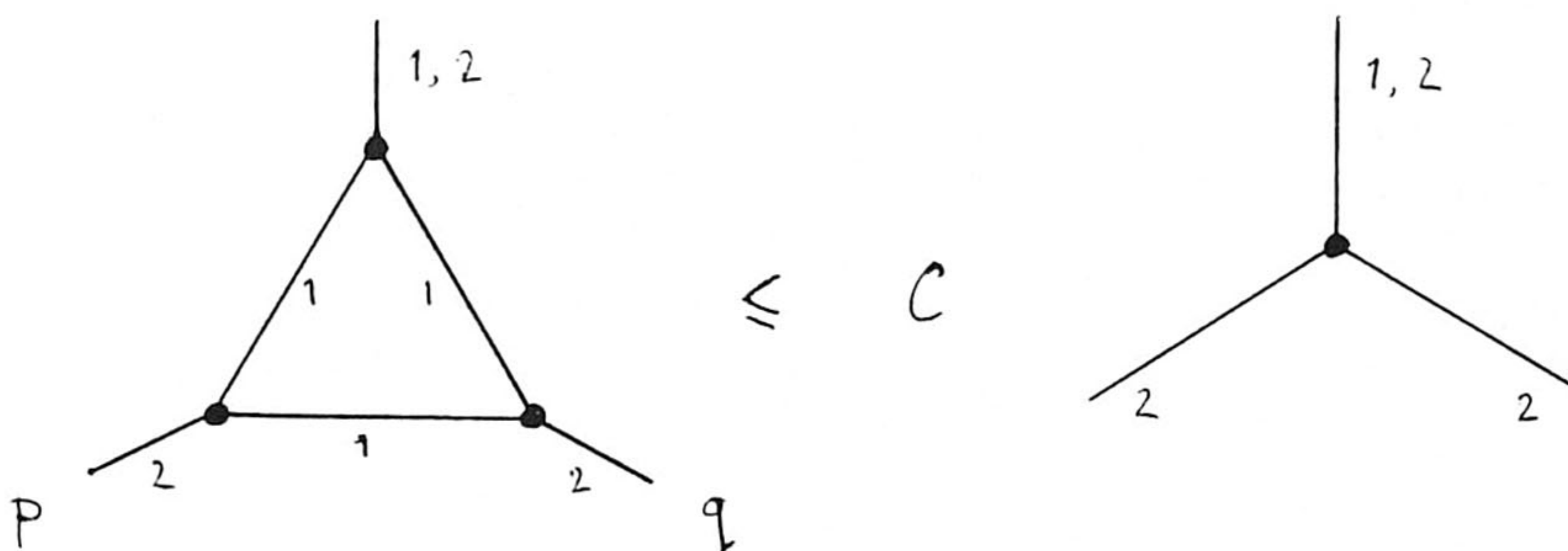
Fig. 9: Removal of elementary triangle facets.

$E_1 = 1$ or o. We write

$$\alpha_1 = \alpha \quad \text{or} \quad \beta - 1 \qquad (8.4)$$

to cover both cases. Now let us replace the vertex functions by bounds that depend only on the momenta of the internal lines:

$$\left(\max(|k|,|k+p|,|p|)\right)^{\gamma} \leqslant R(\gamma)\left(|k|^{\gamma} + |k+p|^{\gamma}\right) \, , \qquad (8.5)$$

with $\quad \gamma = 1+3\alpha \; ; \; R(\gamma) = 2^{3\alpha} \, ,$

or $\qquad \gamma = \beta + 2\alpha \; ; \; R(\gamma) = 1 \; .$ (8.6)

The integral over the loop momentum is then bounded by 8 terms all of the form

$$R \int d^4k \; (k^2)^{-\delta_1} (k+p)^{-2\delta_2} \; (k-q)^{-2\delta_3} \; , \tag{8.7}$$

where for a moment we ignored the mass term. It can be added easily later. We have convergence for all integrals:

$$Z = 2 \sum \delta - 4 = 1 - 2\beta - \alpha_1 > o \; . \tag{8.8}$$

and

$$\delta_1 \geqslant 1 + \alpha - \tfrac{1}{2}(2\alpha + \beta) - \tfrac{1}{2}(1 + 2\alpha + \alpha_1) = \tfrac{1}{2}(1 - 2\alpha - \alpha_1 - \beta) \; ; \tag{8.9}$$

The integral (8.7) can be done using Feynman multiplicators:

$$\frac{R\pi^2 \Gamma(\Sigma\delta - 2)}{\Gamma(\delta_1)\Gamma(\delta_2)\Gamma(\delta_3)} \int_0^1 dx_1 dx_2 dx_3 \; \frac{\delta(\Sigma x - 1) \; x_1^{\delta_1 - 1} \; x_2^{\delta_2 - 1} \; x_3^{\delta_3 - 1}}{\left(p^2 x_2 x_3 + q^2 x_3 x_1 + (p+q)^2 x_1 x_2\right)^{\sum_i \delta_i - 2}} \tag{8.10}$$

Now if $|p| \geqslant |q| \geqslant |p+q|$ (the other cases can be obtained by permutation) then $|q| \geqslant \tfrac{1}{2}|p|$, so our integrals are bounded by

$$C \left[\max(|p|, |q|, |p+q|) \right]^{-\tfrac{1}{2}Z} \tag{8.11}$$

where C is the sum of integrals of the type

$$\frac{\pi^2 \Gamma(\Sigma\delta - 2)}{\Gamma(\delta_1)\Gamma(\delta_2)\Gamma(\delta_3)} \int_0^1 dx_1 dx_2 dx_3 \; \frac{\delta(\Sigma x - 1) \; x_1^{\delta_1 - 1} \; x_2^{\delta_2 - 1} \; x_3^{\delta_3 - 1}}{(x_1 x_2 + \tfrac{1}{2} x_1 x_3)^{\tfrac{1}{2}Z}} \tag{8.12}$$

which can be further bounded (replacing $x_1 x_2$ by $\tfrac{1}{2} x_1 x_2$) by

$$C \leqslant \sum \frac{2^{\Sigma\delta - 2} \; \pi^2 \; \Gamma(\Sigma\delta - 2)\Gamma(2 - \delta_1)\Gamma(2 - \delta_2 - \delta_3)}{\Gamma(\delta_1) \; \Gamma(\delta_2 + \delta_3)} \; , \tag{8.13}$$

if all integrals converge, of course. All entries in the Γ

functions must be positive. In particular, we must have

$$2 - \delta_2 - \delta_3 = \delta_1 - \tfrac{1}{2}Z > o \ . \tag{8.14}$$

Now with (8.8) and (8.9) this corresponds to the condition:

$$\beta > 2\alpha \ , \tag{8.15}$$

this is the extra restriction on the coefficients α and β to be
combined with (5.12), and which we already alluded to in the end
of sect. 5. A good choice may be

$$\alpha = 0.1 \ , \ \beta = 0.3 \ . \tag{8.16}$$

We conclude that we proved the bound of Fig. 9, if α and β have
values such as (8.16), and the number C in Fig. 9 is bounded by
the sum of eight finite numbers in the form of eq. (8.13).

9. QUADRANGLES

We continue removing triangular facets from our diagram,
replacing then by single 3-vertices, following the prescriptions
of the previous sections. We get fewer and fewer loops, at the
cost of at most a factor C for each loop. Either we end up with a
tree diagram, in which case our argument is completed, or we may
end up with a diagram that can still be arbitrarily large but only
contains larger facets. According to sect. 7 there must be
quadrangles and/or pentagons among these.

Before concentrating on the quadrangles we must realize that
there still may be larger subgraphs with only three external lines.
In that case we consider those first: a minimal triangular sub-
graph is a triangular subgraph that contains no further triangular
subgraphs. If our diagram contains triangular subgraphs then we
first consider a minimal triangular subgraph and attack
quadrangles (later pentagons) in these. Otherwise we consider the
quadrangles inside the entire diagram.

Let us again replace as many composite propagators (•——2——•)
by single dressed propagators (•——1——•) as allowed by ineq. (8.1)
for each subgraph. Then one can argue that as a result we must get
at least one quadrangle somewhere whose own propagators are all of
the elementary type (•——1——•), not composite (•——2——•). This is
because facets with composite propagators now must be adjacent to
4-leg subgraphs (elementary facets or more complicated), and then
these in turn must have facet(s) with elementary propagators. Also
(although we will not really need this) one may argue that there
will be quadrangles with not more than one external composite
propagator, the others elementary (the one exception is the case
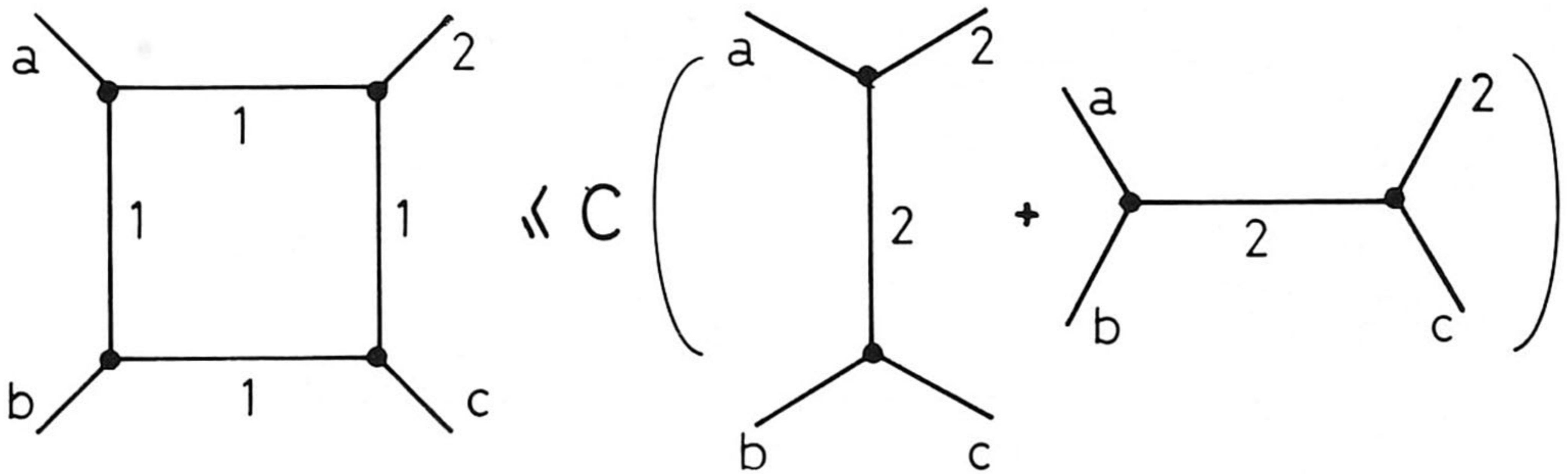when one of the adjacent quadranglular subgraphs has itself only

Fig. 10. Inequality for quadrangles. a, b and c may each be 1 or 2.

pentagons, but that case will be treated in the next section). As a result of these arguments, of all inequalities of the type given in Fig. 10 we only need to check the case that only one external propagator is composite, $a = b = c = 1$.

But in fact they hold quite generally, also in the other cases. This is essentially because of the careful construction of the effective Feynman rules of type IV in Fig. 5.

Rather than presenting the complete proof of the inequalities of Fig. 10 (5 different configurations) we will just present a simple algorithm that the reader can use to prove and understand these inequalities himself. In general we have integrals of the form

$$\int d^4k \ \prod_i \frac{1}{\left|k-p_i\right|^{2\delta_i}} \ . \tag{9.1}$$

We could write this as a diagram in Fig. 11, where the δ_i at the propagators now indicate their respective powers. The vertices are here ordinary point-vertices, not the type IV rules. Now write

$$\frac{1}{|k-p_1|^{\omega_2}|k-p_2|^{\omega_2}} \leq \frac{A(\omega_1,\omega_2)}{|p_1-p_2|^{\omega_2}|k-p_1|^{\omega_1}} + \frac{A(\omega_2,\omega_1)}{|p_1-p_2|^{\omega_1}|k-p_2|^{\omega_2}} \tag{9.2}$$

with

$$A(\omega_1,\omega_2) = \max\left[1, \left(\left(\frac{\omega_1}{\omega_1+\omega_2}\right)^{\omega_1} + \left(\frac{\omega_2}{\omega_1+\omega_2}\right)^{\omega_2}\right)^{-1}\right] . \tag{9.3}$$

Inserted in a diagram, this is the inequality pictured in Fig. 11.

a

b
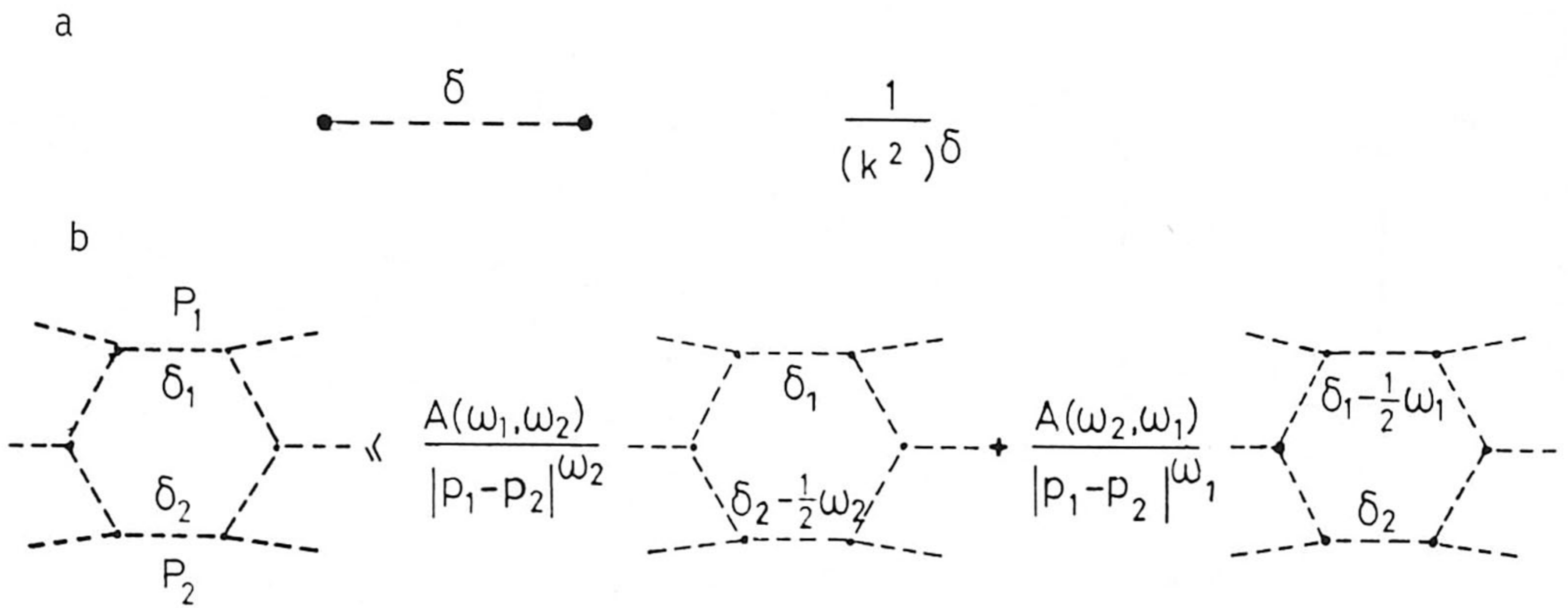
Fig. 11. a) Definition of a dotted propagator. Its vertices are just 1.
b) Extraction of a power of an external momentum.

We use it for instance when $p_1 - p_2$ is the largest momentum of all channels, and if

$$\omega_1 \leqslant 2\delta_1 \; ; \; \omega_2 \leqslant 2\delta_2 \; ; \; \omega_i < Z \; , \tag{9.4}$$

where Z is the degree of convergence of the diagram: $Z = 2\Sigma\delta_i - 4$. We continue making such insertions, everytime reducing the diagrams to a convenient momentum dependent factor times a less convergent diagram. Finally we may have

$$Z < 2\delta_1 \; , \; Z < 2\delta_2 \; , \tag{9.5}$$

for two of its propagators. Then we use the inequality pictured in Fig. 12:

$$\int d^4k \prod_i (k - p_i)^{-2\delta_i} \leqslant C|p_1 - p_2|^{-Z} \; . \tag{9.6}$$

Notice that in (9.5) we have a strictly unequal sign, contrary to ineq. (9.4). This C can be computed using Feynman multiplicators,
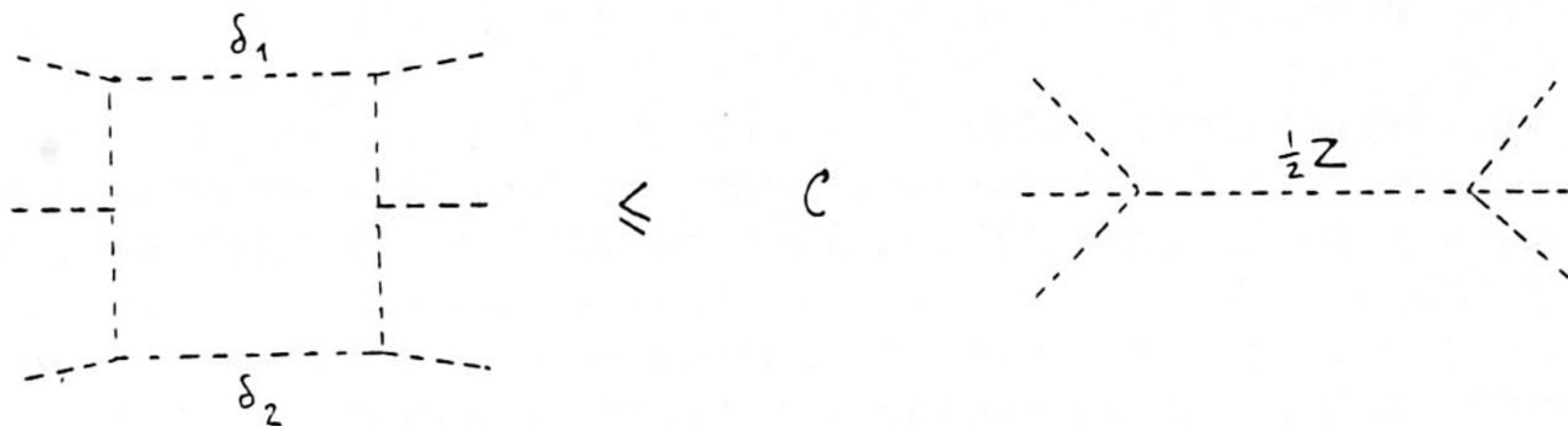
Fig. 12. Inequality holding if $\delta_{1,2}$ are strictly larger than $\frac{1}{2}Z$ (ineqs. (9.4), (9.5)).

much like in the previous section. We get

$$C \leqslant \frac{\pi^2 \Gamma(\frac{1}{2}Z)}{\Gamma(2-\frac{1}{2}Z)} \prod_{i=1,2} \frac{\Gamma(\delta_i - \frac{1}{2}Z)}{\Gamma(\delta_i)} . \tag{9.7}$$

We see that ineqs. (9.2) and (9.6) have essentially the same effect: if two propagators have a power larger than a certain coefficient they allow us to obtain as a factor a corresponding "propagator" for the momentum in that particular channel. This is how proving the ineqs. of Fig. 10 can be reduced to purely algebraic manipulations. We discovered that ineq. (8.15) is again crucial. We notice that if the internal propagators of the quadrangle were elementary ones then the superficial degree of convergence of any of the other subgraphs of our diagram may change slightly, since in eq. (5.10) $\beta > 2\alpha$, but the left hand side of eq. (5.11) remains unchanged, because

$$\Delta E_1 = -2\Delta E_2 , \tag{9.8}$$

so our condition that all subgraphs be convergent remains fulfilled after the substitution of the inequalities of Fig. 10.

However, if one of the internal lines of the quadrangle had been a composite one (•——2——•), then a subgraph would become more divergent, because we are unable to continue our scheme with something like a three-particle composite propagator (•——3——•). A crucial point of our argument is that we will never really need such a thing, if we attack the quadrangle subgraphs in the right order.

10. PENTAGONS. CONVERGENCE OF THE SKELETON EXPANSION

As stated before, the order in which we reduce our diagram

into a tree diagram is:

1) remove triangular facets;
2) remove triangular subgraphs if any. By complete induction we
   prove this to be possible. Take a minimal triangular subgraph
   and go to 3;
3) remove quadrangular facets as far as possible. If any cannot be
   removed because of a crucial composite propagator in them, then
4) remove qudrangular subgraphs. After that we only have to
5) remove the pentagons.
6) If we happened to be dealing with a subgraph by branching at
   point 2 or 3, then by now that will have become a tree graph,
   because of the theorem in sect. 7. Go back to 1.

   We still must verify point 5. If indeed our whole diagram
contains pentagons then we can replace all propagators by
elementary ones. But if we had branched at steps 2 or 3 then the
subgraphs we are dealing with may still have composite external
propagator(s). In that case it is easy to verify that there will
be enough pentagons buried inside our subgraphs that do not need
composite external lines. In that case we apply directly the
inequality of Fig. 13. The procedure for proving Fig. 13 is
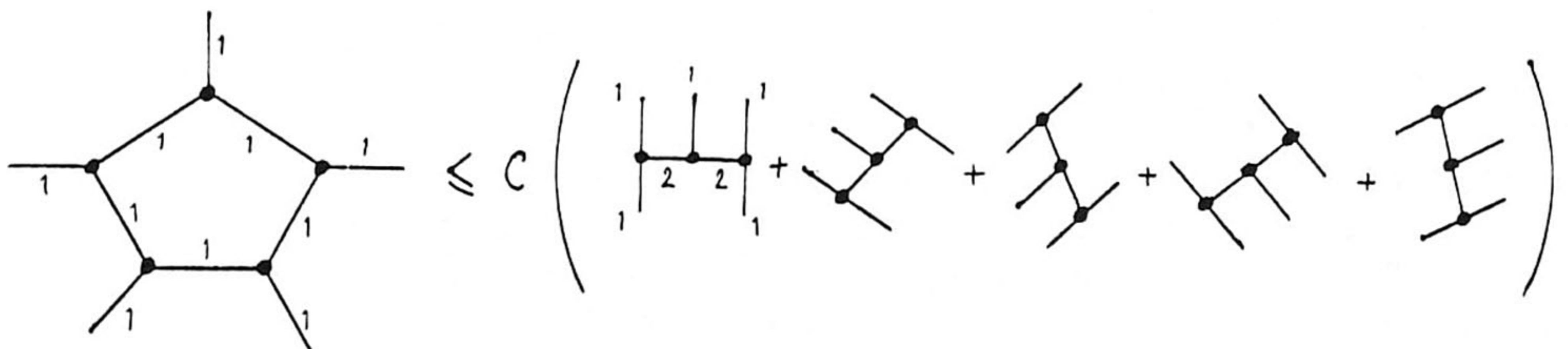
Fig. 13. Inequality for pentagons.

exactly as described for the quadrangles in the previous section.
Again the degree of divergence of any of the adjacent subgraphs
has not changed significantly. This now completes our proof by
induction that any planar skeleton diagram with 5 external lines
is equal to C^L times a diagram with type IV Feynman rules, where C
is limited to fixed bounds. Since also the number of diagrams is
an exponential function of L we see that for this set of graphs
perturbation expansion in g has a finite radius of convergence.
The proof given here is slightly more elegant than in Ref. 11, and
also leads to tree graph expressions that are more useful for our
manipulations.

If the diagram has 6 or more external lines then still a number of facets may be left, limited by ineq. (7.10), all having 6 or more propagators. If we wish we can still continue our procedure for these but that would be rather pointless: having a limited number of loops the diagram is finite anyhow. The difficulty would not so much be that no inequalities for hexagons etc. could be written down; they certainly exist, but our problem would be that the corresponding number C would not obviously be bounded by one universal constant. This is why our procedure would not work for nonplanar theories where ineq. (7.10) does not hold. In the non-planar case however similar theorems as ours have been derived[6].

11. BASIC GREEN FUNCTIONS

The conclusion of the previous section is that if we know the "basic Green functions", with which we mean the two- three- and four-point functions, and if these fall within the bounds given in Table 1, then all other Green functions are uniquely determined by a convergent sum. Clearly we take the value for the bound g^2 for the coupling constant (ineq. (5.9)) as determined by the inverse product of the coefficient C_2 found in sect. 6 and the maximum of the coefficients in the ineqs. pictured in Figs. 9, 10 and 13, times a combinatorial factor.

Now we wish not only to verify whether these bounds are indeed satisfied, but also we would like to have a convergent calculational scheme to obtain these basic Green functions. One way of doing this would be to use the Dyson-Schwinger equations. After all, the reason why those equations are usually unsoluble is that they contain all higher Green functions for which some rather unsatisfactory cut-off would be needed. Now here we are able to re-express these higher Green functions in terms of the basic ones and thus obtain a closed set of equations.

These Dyson-Schwinger equations however contain the bare coupling constants and therefore require subtractions. It is then hard to derive bounds for the results which depend on the difference between two (or more) divergent quantities. We decided to do these subtractions in a different way, such that only the finite, renormalized basic Green functions enter in our equations, not the bare coupling constants, in a way not unlike the old "bootstrap" models. Our equations, to be called "difference equations" will be solved iteratively and we will show that our iteration procedure converges. So we start with some *Ansatz* for the basic Green functions and derive from that an improved set of values using the difference equations. Actually this will be done in various steps. We start with assuming some function g(x) for the *floating coupling constant*, where x is the momentum in the maximal channel (see Table 1):

$$x = \max_{i,j} |p_i - p_j| \,, \tag{11.1}$$

and a set of functions $g_{(i)}(x)$ with

$$g(x) \underset{\text{def}}{=} \max_i |g_{(i)}(x)| \,. \tag{11.2}$$

Here $g_{(i)}(x)$ is the set of independent numbers that determined the basic Green function at their "symmetry point":

$$|p_i - p_j| = x \quad \text{for all } i,j \,. \tag{11.3}$$

The index i in $g_{(i)}$ then simply counts all configurations in (11.3). With "independent" we mean that in some gauge theories we assume that the various Ward-Slavnov-Taylor[13] identities among the basic Green functions are fulfilled. This is not a very crucial point of our argument so we will skip any further discussion of these Ward or Slavnov-Taylor identities.

If the values of the basic n-point Green functions (n = 3 or 4) at their symmetry points are $A_i(x)$, then the relation between A_i and g_i is:

$$A_{3i}(x) = \kappa_{i\mu}^j \, p_{j\mu} \, Z^{-3/2}(x) \, g_{ij}(x)$$
$$A_{4i}(x) = Z^{-2}(x) \, g_{4i}^2(x) \,, \tag{11.4}$$

where $\kappa_{i\mu}^j$ are coefficients of order one, and $Z(x)$ is defined in (5.1) and (5.2). (We ignore for a moment the case of super-renormalizable couplings.) Our first Ansatz for $g_i(x)$ is a set of functions that is bounded by (11.2), with $g(x)$ decreasing asymptotically to zero for large x as dictated by the lowest order term(s) of the renormalization group equations. We will find better equations for $g_i(x)$ as we go along. In any case we will require

$$\left| \frac{xd}{dx} g_i(x) \right| \leqslant \tilde{\beta} \, g^3(x) \tag{11.5}$$

for some finite coefficient $\tilde{\beta}$.

Our first *Ansatz* for the basic Green functions away from the symmetry points will be even more crude. All we know now is that they must satisfy the bounds of Table 1. In general one may start with choosing (11.4) to hold evenaway from the symmetry points, and

$$x = \max_{i,j} |p_i - p_j| \,. \tag{11.6}$$

After a few iterations we will get values still obeying the bounds of Table 1, and with *uncertainties* also given by Table 1 but K_i replaced by coefficients δK_i. Thus we start with

$$\delta K_i^{(0)} = K_i \ . \tag{11.7}$$

We will spiral towards improved *Ansätze* for the basic Green functions in two movements:

i) the "small spiral" is the use of difference equations to obtain improved values at exceptional momenta, *given the values $g_i(x)$ at the symmetry points*. These difference equations will be given in the next section.

ii) The "second spiral" is the use of a variant of the Gell-Mann-Low equation to obtain improved functions $g_i(x)$ from previous Ansätze for $g_i(x)$, making use of the convergent "small spiral" at every step. What is also needed at every step here is a set of integration constants determining the boundary condition of this Gell-Mann-Low equation. It must be ensured that these are always such that $g(x)$ in ineq. (11.2) remains bounded:

$$g(x) < g_0 \ ,$$

where g_0 is limited by the coefficients K_i and the various coefficients C from sects. 6, 8, 9 and 10, as in ineq. (5.9).

12. DIFFERENCE EQUATIONS FOR BASIC GREEN FUNCTIONS

The Feynman rules of our set of theories must follow from a Lagrangian, as usual.
For brevity we ignore the Lorentz indices and such, because those details are not of much concern to us. Let the dressed propagator be

$$P(p) = -G_2^{-1}(p) \ , \tag{12.1}$$

and let the corresponding zeroth order expressions be indicated by adding a superscript o. In massive theories:

$$P^0(p) = (p^2+m^2)^{-1} = -G_2^{0-1}(p) \ . \tag{12.2}$$

Define

$$G_2(p+k) - G_2(p) = G_{2\mu}(p|k)k_\mu \ , \tag{12.3}$$

so that

$$P(p+k) - P(k) = P(p+k)G_{2\mu}(p|k)k_\mu P(p) \ . \tag{12.4}$$

This gives us the "Feynman rule" for the difference of two dressed

Fig. 14. Feynman rule for the difference of two dressed propagators. The 3-vertex at the right is the function $G_{2\mu}(p|k)$.

Fig. 15. Difference equation (12.6) for $G_{2\mu}$.
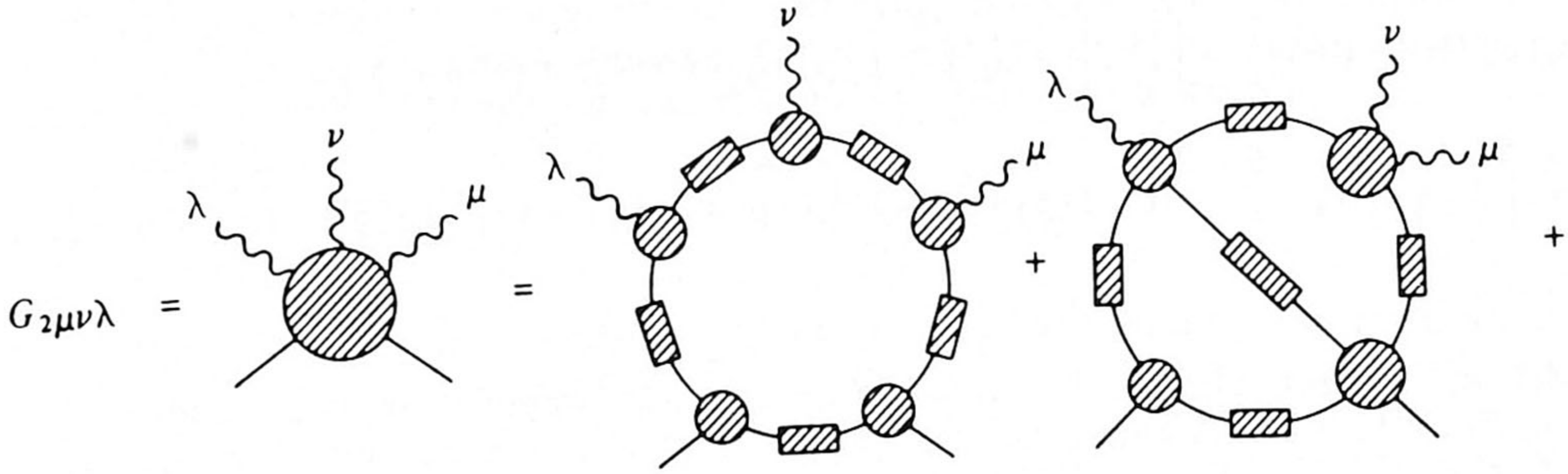
Fig. 16. Some arbitrarily chosen terms in the skeleton expansion
for $G_{2\mu\nu\lambda}$.

propagators, depicted in Fig. 14. (Note that, in this section only,
p and k denote external line momenta, not external loop momenta.)

We have also this Feynman rule for bare propagators. There
$G^0_{2\mu}$ follows directly from the Lagrangian:

$$G^0_{2\mu} = - 2p_\mu - k_\mu .$$ (12.5)

Continuing this way we define

$$G_{2\mu}(p|k+q) - G_{2\mu}(p|k) = G_{2\mu\nu}(p|k|q)q_\nu ,$$ (12.6)

with

$$G^0_{2\mu\nu} = -\delta_{\mu\nu} .$$ (12.7)

In Feynman graphs this is sketched in Fig. 15. Differentiating
once more we get

$$G_{2\mu\nu}(p|k|q+r) - G_{2\mu\nu}(p|k|q) = G_{2\mu\nu\lambda}(p|k|q|r)r_\lambda .$$ (12.8)

Of course $G_{2\mu\nu\lambda}$ can be computed formally in perturbation ex-
pansion. The rules for computing the new Green functions G_μ, $G_{\mu\nu}$,
$G_{\mu\nu\lambda}$ are easy to establish. Let p_1 be one of the external loop mo-
menta as defined in eq. (5.3). For a Green function $G(p_1)$ we have

$$G(p_1) = \int \ldots \int dq_i \; f_1(p_1+q_1)f_2(p_1+q_2) \ldots f_t(p_1+q_t).F ,$$
(12.9)

where $f_i(q_i)$ are bare vertex and/or propagator functions adjacent
to the external facet labeled by 1. The remainder F is independent
of p_1. We write

$$G(p_1+k) - G(p_1) = \int \ldots \int F \, dq \left(\prod_1^t f(p_1+q_i+k) - \prod_1^t f(p_1+q_i) \right)$$

$$= \int \ldots \int F \, dq \sum_{s=1}^t \prod_1^{s-1} f(p_1+q_i+k) \left(f(p_1+q_s+k) - f(p_1+q_s) \right) \prod_{s+1}^t f(p_1+q_i),$$

$$(12.10)$$

which is just the rule for taking the difference of two products. We find the difference of two *dressed* Green functions G in terms of the difference of *bare* functions f. Therefore the "Feynman rules" for the diagrams at the right hand sides of Figs. 14, 15 and the l.h.s. of Fig. 16 consist of the usual combinatorial rules with new bare vertices given by the eqs. (12.5) and (12.7). These bare vertices occur only at the edge of the diagram.

We see that the power counting rules for divergences in $G_{2\mu\nu\lambda}$ are just as in 5-point functions in gauge theories. Since the global degree of divergence is negative we can expand in skeleton graphs. See Fig. 16, in which the blobs represent ordinary dressed propagators and dressed vertices or dressed functions G_μ and $G_{\mu\nu}$.

Notice that one might also need $G_{3\mu}(p_1,p_2|k)$ defined by

$$G_3(p_1,p_2+k) - G_3(p_1,p_2) = G_{3\mu}(p_1,p_2|k) \cdot k_\mu \ . \qquad (12.11)$$

In short, the skeleton expansion expresses $G_{2\mu\nu\lambda}$ but also $G_{3\mu\nu}$ etc. in terms of the few basic functions $G_{2\mu}$, $G_{2\mu\nu}$, $G_{3\mu}$ and the basic Green functions $G_{2,3,4}$. Also the function $G_{4\mu}$, defined similarly, can thus be expressed. The corresponding Feynman rules should be clear and straightforward.

We conclude that the basic Green functions can in turn be expressed in terms of skeleton expansions, and, up to overall constants, these equations, if convergent, determine the Green functions completely. Notice that we never refer to the bare Lagrangian of the theory, so, perhaps surprisingly, these sets of equations are the same for all field theories. The difference between different field theories only comes about by choosing the integration constants differently.

Planarity however was crucial for this chapter, because only planar diagrams have well defined "edges": the new vertices only occur at the edge of a diagram.

13. FINDING THE BASIC GREEN FUNCTIONS AT EXCEPTIONAL MOMENTA (THE "SMALL SPIRAL")

In this section we regard the basic Green functions at their symmetry points as given, and use the difference equations of

Sect. 12 to express the values at exceptional momenta in terms of these. If p_i-p_j is the momentum flowing through the planar channel ij, then in our difference equations we decide to keep

$$\mu = \max_{i,j} |p_i-p_j| \qquad (13.1)$$

fixed. So the left hand side of our difference equations will show two Green functions with the same value for μ, one of which may be exceptional and the other at its symmetry point, and therefore known. (We use the concept of "exceptional momenta" as in ref. 14.)

Now the right hand side of these difference equations show a skeleton expansion of diagrams which of course again contain basic Green functions, also at exceptional momenta. But these only come in combinations of higher order, and the effect of exceptional momenta is relatively small, so at this point one might already suspect that when these equations are used recursively to determine the exceptional basic Green functions then this recursion might converge. This will indeed be the case under certain conditions as we will show in sect. 15.

Our iterative procedure must be such that after every step the bounds of Table 1 again be satisfied. This will be our guide to define the procedure. First we take the 4-point functions, and consider all cases of Table 1 separately.

The right hand side of our difference equations (Fig. 16) contains a skeleton expansion to which we apply the theorem mentioned in the end of sect. 5 and proven in sects. 5-10: the skeleton expansion for any 5-point Green function converges and is bound by tree diagrams constructed with type IV Feynman rules. Since the 5-point functions in Fig. 16 are irreducible, the internal lines in the resulting tree graph will always be composite propagators, as in the r.h.s. of Fig. 13. So we simply apply the type IV Feynman rules for 5 tree graphs to obtain bounds on the 5-point function in various exceptional regions of momentum space. Table 2 lists the results.

The power of $g^2(A_3)$ in the table applies where we consider the function $G_{4\mu}$. The other functions $G_{3\mu\nu}$ and $G_{2\mu\nu\lambda}$ have one and zero powers of $g(A_3)$, respectively. In front of all this comes a power series of the form

$$\sum_{n=1}^{\infty} c^n g_0^{2n} = Cg_0^2(1-Cg_0^2)^{-1} , \qquad (13.2)$$

which converges provided that

Table 2

Bounds for the irreducible 5-point function at some exceptional momentum values.

$(((12)_1 \ 53)_2 \ 4)_3$	$\prod_i Z_{ii+1}^{-\frac{1}{2}} \ A_1^{-\alpha} \ A_2^{-1+\alpha-\beta} \ A_3^{\beta} \ g^2(A_3)$
$((12)_1 \ 5 \ (34)_2)_3$	$\prod_i Z_{ii+1}^{-\frac{1}{2}} \ A_1^{-\alpha} \ A_2^{-\alpha} \ A_3^{2\alpha-1} \ g^2(A_3)$
$(((513)_1 \ 2)_2 \ 4)_3$	$\prod_i Z_{ii+1}^{-\frac{1}{2}} \ A_1^{-1-2\beta} \ A_2^{\beta} \ A_3^{\beta} \ g^2(A_3)$
$((135)_1 \ (24)_2)_3$	$\prod_i Z_{ii+1}^{-\frac{1}{2}} \ A_1^{-1-2\beta} \ A_3^{2\beta} \ g^2(A_3)$ if $A_2 > A_1$
$((1235)_1 \ 4)_2$	$\prod_i Z_{ii+1}^{-\frac{1}{2}} \ A_1^{-1-\beta} \ A_2^{\beta} \ g^2(A_3)$

$$g_0 = \max_\mu |g(\mu)| < C^{-\frac{1}{2}} . \tag{13.3}$$

We now write an equation such as (12.8) as follows:

$$\widetilde{G}_4\{(((12)_1 \ 3)_2 \ 4)_3\} = G_4\{((523)_2 \ 4)_3\} +$$
$$+ (p_1-p_5)_\mu \ G_{4\mu}\{(((12)_1 \ 53)_2 \ 4)_3\} , \tag{13.4}$$

where $r = p_1-p_5$. In this and following expressions the tilde ($\sim$) indicates which quantities are being replaced by new ones in the iteration procedure.

If the Ansatz holds for $G_4\{((523)_2 \ 4)_3\}$ then the new exceptional function will obey

$$|\widetilde{G}_4\{(((12)_1 \ 3)_2 \ 4)_3\}| \leqslant K_6^2 (Z_{45}Z_{52}Z_{23}Z_{34})^{-\frac{1}{2}} \left(\frac{A_3}{A_2}\right)^\beta g^2(A_3) +$$
$$+ (Z_{45}Z_{12}Z_{23}Z_{34})^{-\frac{1}{2}} \frac{Cg_0^2}{1-Cg_0^2} g^2(A_3) \left(\frac{A_2}{A_1}\right)^\alpha \left(\frac{A_3}{A_2}\right)^\beta . \tag{13.5}$$

Choosing $\quad \dfrac{Cg_0^2}{1-Cg_0^2} \equiv \gamma \tag{13.6}$

and considering that to a good approximation (since $|p_1-p_5| \ll |p_4-p_5|$):

$$Z_{45} = Z_{41} , \tag{13.7}$$

we find

$$|\tilde{G}_4\{(((12)_1 \ 3)_2 \ 4)_3\}| \leqslant (Z_{12}Z_{23}Z_{34}Z_{41})^{-\frac{1}{2}} \ g^2(A_3)\left(\frac{A_2}{A_1}\right)^\alpha \left(\frac{A_3}{A_2}\right)^\beta \ .$$

$$\cdot \left(\gamma + \left(\frac{Z_{12}}{Z_{52}}\right)^{\frac{1}{2}} \left(\frac{A_1}{A_2}\right)^\alpha K_6^2\right) \ . \tag{13.8}$$

What is now needed is a bound for the last term in (13.8). Let

$$x_{12} = |p_{12}|/m \geqslant 1 \tag{13.9}$$

(remember that $|p|$ stands for $\sqrt{p^2+m^2}$),
and

$$f(x_{12}) = (\log(1+x_{12})^{\sigma/2} \cdot x_{12}^\alpha \ , \tag{13.10}$$

where σ is defined in (5.2).
When

$$x_{12} > \exp \ (-\sigma/2\alpha) = x_0 \tag{13.11}$$

this f is an increasing function, so that if

$$x_0 m \leqslant A_1 < A_2 \tag{13.12}$$

then

$$\frac{f(x_{12})}{f(x_{52})} < 1 \ . \tag{13.13}$$

The range $1 \leqslant x \leqslant x_0$ is compact, so there exists a finite number L
such that

$$\frac{f(x_{12})}{f(x_{52})} \leqslant L \tag{13.14}$$

as soon as

$$x_{12} < x_{52} \ . \tag{13.15}$$

So we find that after one iteration given by (13.4), the new K_2
coefficient satisfies

$$K_2^2 \leqslant \gamma + K_6^2 L \ . \tag{13.16}$$

Similarly we derive

$$K_7^2 \leqslant \gamma + L \ ,$$ (13.17)

when the difference equation is used to express $\widetilde{G}\{((12)_1 \ 34)_2\}$ in terms of $G\{(5234)_2\}$. Also we use

$$\widetilde{G}_4\{((12)_1 \ (34)_2)_3\} = G_4\{(52(34)_2)_3\} +$$

$$+ \ (p_1 - p_5)_\mu \ G_{4\mu}\{((12)_1 \ 5(34)_2)_3\} \ ,$$ (13.18)

to find that after one step

$$K_3^2 \leqslant \gamma + K_7^2 L \leqslant \gamma + \gamma L + L^2 \ ;$$ (13.19)

and for the three-point function

$$K_1 \leqslant K_7^2 + L \leqslant \gamma + 2L \ .$$ (13.20)

The remaining coefficients K_{4-6} must be computed in a slightly different way. Consider K_4. We replace p_1 by p_5 now in such a way that

$$|p_5 - p_3| \simeq 2|p_1 - p_3| \ ; \qquad A_1 \rightarrow 2A_1$$ (13.21)

and work with induction. Write

$$\widetilde{G}_4\{(((13)_1 \ 2)_2 \ 4)_3\} = \widetilde{G}_4\{(((53)_1 \ 2)_2 \ 4)_3\}$$

$$+ \ (p_1 - p_5)_\mu \ G_{4\mu}\{(((513)_1 \ 2)_2 \ 4)_3\} \ .$$ (13.22)

Inspecting Tables 1 and 2 we find now

$$K_4^2 = \max\left(K_6^2 \ , \ \frac{\gamma}{1-2^{-2\beta}}\right) \ .$$ (13.23)

Applying the same technique we compute the fifth exceptional configuration of Table 1. We separate p_1 from p_3 until $A_1 \rightarrow A_2$. Then we separate alternatively p_2 from p_4 and p_1 from p_3 keeping $A_1 \simeq A_2$. This makes the rate of convergence slightly slower:

$$K_5^2 = \frac{2\gamma}{1-2^{-2\beta}} \ .$$ (13.24)

Finally K_6 is found by widening the separation between p_1, p_2 and p_3 in successive steps of factors of 2:

$$\widetilde{G}_4\{((123)_1 \ 4)_2\} = \widetilde{G}_4\{((563)_1 \ 4)_2\}$$ (13.25)

$$+ \ (p_5 - p_1)_\mu \ G_{4\mu}\{((1235)_1 \ 4)_2\} + (p_6 - p_2)_\mu \ G_{4\mu}\{((2356)_1 \ 4)_2\} \ ,$$

where

$$|p_5 - p_6| = |p_3 - p_6| = |p_5 - p_3| \simeq 2|p_1 - p_2| \ . \tag{13.26}$$

We find

$$|\widetilde{G}_4\{((123)_1 \ 4)_2|\} \leqslant \gamma Z(A_1)^{-1} \ Z(A_2)^{-1} \left(\frac{A_2}{A_1}\right)^{\beta} \ .$$

$$\sum_{n=1}^{2 \log (A_2/A_1)} \left(2^{-\beta n} \cdot 2 \ \frac{Z(A_1)}{Z(2^n A_1)}\right) + |G_4\{(1234)_2\}| \ . \tag{13.27}$$

The sum can certainly be bounded:

$$\sum \leqslant L' \leqslant 2L(1-2^{\alpha-\beta})^{-1} \ . \tag{13.28}$$

Therefore

$$K_6^2 \leqslant \max(1, \gamma L') \ . \tag{13.29}$$

Thus all coefficients K_i have bounds that will be obeyed everywhere in the "small spiral" induction procedure. Note that these coefficients would blow up if $\alpha, \beta \to o$. In particular in (13.11) we need $\alpha > o$. Only if $g_0^2 \to o$ we can let $\alpha, \beta \to o$. It will be clear from the above arguments that our bounds are only very crude. Our present aim was to establish their existence and not to find optimal bounds.

In sect. 15 we show that the "small spiral" of iterations for the exceptional Green functions, given the non-exceptional ones in (13.27), actually converges geometrically.

14. NON-EXCEPTIONAL MOMENTA (THE "SECOND SPIRAL")

In order to formulate the complete recursion procedure for determining the basic Green functions we need relations that link these Green functions at different symmetry points. Again the difference equations are used:

$$G_4(p_1 \ldots p_4) = G_4(2p_1, p_2 p_3 p_4) - p_\lambda G_{4\lambda}(p_1, 2p_1, p_2 p_3 p_4)$$

$$= \ldots = G_4(2p_1, \ldots, 2p_4) - \sum_{i=1}^{4} p_{i\lambda} G_{4\lambda}(p_1^{(i)}, \ldots, p_5^{(i)}) \ . \tag{14.1}$$

Here p_i and $p_j^{(i)}$ are external loop momenta. They are non-exceptional. We use a shorthand notation for (14.1). Writing $p_i^2 \simeq (p_i - p_j)^2 \simeq \mu^2$:

$$G_4(\mu) - G_4(2\mu) = \mu \sum_{i=1}^{4} G_{4\lambda}^{(i)}(2\mu,\mu) \ . \tag{14.2}$$

Similarly we have

$$G_{2,3}(\mu) - G_{2,3}(2\mu) = - \mu \sum_i G_{2,3\lambda}^{(i)}(2\mu,\mu) \ . \tag{14.3}$$

These are just discrete versions of the renormalization group
equations. The right hand side of (14.2), [not (14.3)!] is to be
expanded in a skeleton expansion which contains all basic Green
functions at all μ, also away from their symmetry points. There we
insert the values obtained after a previous iteration. It is our
aim to derive from eq. (14.2) a Gell-Mann-Low equation[1] of the form

$$\frac{\mu \partial}{\partial \mu} g_i(\mu) = - \sum_{\ell=2}^{k} \beta_{ij_1 \cdots j_\ell}^{(\ell)} g_{j_1}(\mu) \cdots g_{j_\ell}(\mu)$$

$$+ |g(\mu)|^N \rho_i(\mu) \ , \tag{14.4}$$

where $\beta^{(\ell)}$ are the first k coefficients of the β function, and they
must coincide with the perturbatively computed β coefficients.
Often (depending on the dimension of the coupling constant) only
odd powers occur so that $k = N-2$ is odd. The rest function ρ must
satisfy

$$|\rho_i(\mu)| \leqslant Q_N \tag{14.5}$$

for some constant $Q_N < \infty$. This inequality must hold in the sense
that $|g(\mu)|^N \rho(\mu)$ must be a convergent expansion in the functions
$g(\mu')$, with

$$\mu' \geqq m \tag{14.6}$$

(so that μ' may be smaller than μ), in such a way that the absolute
value of each diagram contributes to Q_N and their total sum remains
finite.

Now clearly eq. (14.2) is a difference equation, not a differ-
ential equation such as (14.4). Up till now differential equations
were avoided because of infrared divergences. Just for ease of
notation we have put (14.4) in differential form because the
mathematical convergence questions that we are to consider now are
insensitive to this simplification.

Consider the skeleton expansion of $G_{4\lambda}^{(i)}$ in (14.2). At each of
the four external particle lines a factor $g(\mu_i)$ occurs with $\mu_i \geqq \mu$,

so it may seem easy to prove (14.4) from (14.2) with N = 3 or 4. However, we find it more convenient* to have an equation of the form (14.4) with $N \leq 7$, and our problem is that the internal vertices of the $G_{4\lambda}^{(i)}$ might have momenta which are less than μ. We will return to this question later in this section.

In proving the difference equation variant of (14.4) from (14.2) we have to make the transition from G_4 to g^2 and G_3 to g, and this involves the coefficients $Z(\mu)$, associated to the functions G_2, by equations of the form

$$G_2(\mu) = - \mu^2 Z^{-1}(\mu) \quad ;$$

$$G_3(\mu) = \mu Z^{-3/2}(\mu) g_3(\mu) \ ; \tag{14.7}$$

$$G_4(\mu) = Z^{-2}(\mu) g_4^2(\mu) \quad .$$

where g_3, g_4 are just various components of the coupling constant g_i. In the following expressions we suppress these indices i when we are primarily interested in the dependence on μ (= $|p|$ at the symmetry point). Now from (14.2) and (14.3) we find not first order but third order differential equations for G_2, basically of the form

$$\frac{\partial^3}{\partial \mu^3} G_2 = G_{2,\lambda\lambda\lambda} = \mathcal{O}(g^2(\mu) Z^{-1}(\mu)/\mu) \ , \tag{14.8}$$

where $G_{2,\lambda\lambda\lambda}$ is just a shorthand notation for the combination of expandable functions $G_{2,\lambda\mu\nu}$ obtained after taking differences three times. Write

$$U_2(\mu) = - \frac{\partial^2}{\partial \mu^2} G_2(\mu) = - G_{2\lambda\lambda}(\mu) \ , \tag{14.9}$$

then

$$\frac{\mu \partial}{\partial \mu} U_2(\mu) = - \mu G_{2,\lambda\lambda\lambda}(\mu) \ , \tag{14.10}$$

and

$$\mu^2 Z^{-1}(\mu) = \int_m^n (\mu - \mu_1) U_2(\mu_1) d\mu_1 + A\mu + B \ . \tag{14.11}$$

---

* Closer analysis shows that actually N = 3 or 4 is sufficient to prove unique solubility. Only if we wish an exact, non-perturbative definition of the free parameters we need the higher N values. Note that not only Q_N but also g_0 may deteriorate as N increases.

Here A and B are free integration constants; A is usually
determined by Lorentz invariance and B by the mass, fixed to be
equal to m. In lowest order:

$$A = mU_2(m) \quad ; \quad B = -\tfrac{1}{2}m^2U_2(m) \ . \tag{14.12}$$

This strange-looking form of the integration constants is an arti-
fact coming from our substitution of difference equations by
differential equations. Using difference equations we can impose
Lorentz invariance by symmetrization in momentum space, so that
only one (for each particle) integration constant is left: the mass
term. We choose at all stages $\tfrac{1}{2}U_2(m) = Z(m) = 1$.

A convenient way to implement eq. (14.12) is to formally
define $U_2(\mu) = 2$ if $o \leq \mu \leq m$, and replace the lower bound of the
integral in (14.11) by zero. Then after symmetrization: A = B = o.

Equation (14.11) has a linearly convergent integral, whereas
(14.10) is logarithmic. Together they determine the next iterative
approximation to G . In fact we have

$$\mu G_{2,\lambda\lambda\lambda}(\mu) = Z^{-1}(\mu)f(\{g\}) \ , \tag{14.13}$$

and in $f(\{g\})$, Z occurs only indirectly. So the iteration converges
fastest if we replace (14.10) by

$$\frac{\mu\partial}{\partial\mu} \widetilde{U}_2(\mu) = -\frac{Z(\mu)}{\widetilde{Z}(\mu)} G_{2,\lambda\lambda\lambda}(\mu) \ , \tag{14.14}$$

where the tilde denotes the new function $U_2(\mu)$.

One can however also use (14.9) with U_2 replaced by $\widetilde{U}_2$.

We find

$$\frac{\mu\partial}{\partial\mu} Z^{-1} = - \int_{m/\mu}^{1} d\tau(1-\tau)\mu G_{2,\lambda\lambda\lambda}(\tau\mu) \ . \tag{14.15}$$

As stated before, the $\mathcal{O}\left(\dfrac{m}{\mu}\right)$ terms have been removed by symmetri-
zation.

This equation allows us to remove the Z factors from the
functions $G_{3,4}$ and arrive at first order renormalization group
integrodifferential equations for $g_i(\mu)$.

For the 3-point functions we must write

$$U_3(\mu) = G_{3,\lambda}(\mu) = \frac{\partial G_3}{\partial\mu} \ ,$$

$$\frac{\mu \partial}{\partial \mu} U_3(\mu) = \mu G_{3,\lambda\lambda}(\mu) \ , \tag{14.16}$$

$$G_3(\mu) = \int_m^\mu \mu U_3(\mu) d\mu + C_3 \ , \tag{14.17}$$

$$\frac{\mu \partial G_3(\mu)}{\partial \mu} = \int_{m/\mu}^1 d\tau \ \mu G_{3,\lambda\lambda}(\tau\mu) \ . \tag{14.18}$$

A potential difficulty in writing down the renormalization group equation even for N = 4 is the convolutions in (14.15) and (14.18) which contain Green functions at lower μ values, and so they depend on $g(\mu')$ with $\mu' < \mu$. So a further trick is needed to derive (14.4). This is accomplished by realizing that the integrals in (14.15) and (14.18) converge linearly in μ. Suppose we require at every iteration step (see eq. 11.5):

$$\left| \frac{\mu \partial}{\partial \mu} g(\mu) \right| \leq \widetilde{\beta} |g(\mu)|^3 \quad \text{and} \quad |g(\mu)| \leq g_0 \tag{14.19}$$

for some $\beta < \infty$, $g_o < \infty$. Then it is easy to show that if $\mu_1 \leq \mu$, then

$$|g(\mu_1)| \leq |g(\mu)| + C \left(\frac{\mu}{\mu_1} \right)^\varepsilon |g^3(\mu)| \ , \tag{14.20}$$

if

$$\varepsilon \geq 3\widetilde{\beta} g_0^2 + \widetilde{\beta}/C \ . \tag{14.21}$$

So with C large enough and g_0 small enough we can make ε as small as we like. Inequality (14.20) is proven by differentiating with μ. This enables us to replace $g(\tau\mu)$ by $g(\mu)$ in (14.15) and (14.18) while the factor $\tau^{-\varepsilon}$ does no harm to our integrals. So we find bounds for $\frac{\mu \partial}{\partial \mu} \widetilde{Z}^{-1}$ and $\frac{\mu \partial}{\partial \mu} \widetilde{G}_3$ in terms of a power series of $g(\mu)$. We must terminate the series as soon as the factors $\tau^{-\varepsilon}$ accumulate to give τ^{-1}. This implies that N must be kept finite, otherwise $g_0 \rightarrow o$.

The same inequality (14.16) is used to go from N = 4 to N = 7 in these equations. If in a skeleton diagram a vertex is not associated with any external line, then it may be proportional to a factor $g(\mu')$ with $\mu' < \mu$. But using (14.16) we see that it may be replaced by $g(\mu)$ at the cost of a factor $(\mu/\mu_1)^\varepsilon$. At most three of these extra factors are needed. If the three corresponding vertices are chosen not to be too far away from one of the external vertices of the diagram (which we can always arrange), then this just corresponds to inserting an extra factor

$\left(\dfrac{p^{ext}}{p_1}\right)^{\varepsilon}$ at an external vertex. We now note that such factors still

leave our integrals convergent. In the ultraviolet of course the
diagrams converge even better than they already did, and in the
infrared our degree of convergence was at least $1-\alpha$ (or $2-\beta$) as
can easily be read off from eq. (5.10): adding the external propa-
gators to any diagram one demands

$$Z + (2+2\alpha)E_1 + 2\beta E_2 < 4(E_1+E_2-1) .\tag{14.22}$$

Thus infrared convergence requires

$$1 - \alpha - T\varepsilon > o \tag{14.23}$$

where $T \lesssim 5$ is the number of times our inequality (14.20) was
applied.

From the above considerations we conclude that an equation of
the form (14.4) can be written down for any finite N, such that Q_N
in inequality (14.5) remains finite. We do expect of course that
Q_N might increase rapidly with N, but then we only want the
equation for $N \leq 7$. We are now in a position to formulate com-
pletely our recursive definition of the Green functions G_2, G_3, G_4
of the theory:

1) We start with a given set of trial functions $G_2(\mu)$, $G_3(\mu)$,
$G_4(\mu)$ for the basic Green functions at their symmetry points. They
determine our initial choice for the floating coupling constants
$g_i(\mu)$ and the functions $Z_i(\mu)$. We require their asymptotic
behaviour to satisfy (5.2), (5.9) and (11.5) (= eq. (14.19)).

2) We also start with an *Ansatz* for the exceptional Green
functions that must obey the bounds of Table 1.

3) Use the difference equations of sect. 13 to improve the
exceptional Green functions (the new values are indicated by a
tilde (~)). These will again obey Table 1 as was shown in sect. 13.
Repeat the procedure. It will converge towards fixed values for the
exceptional Green functions (as we will argue in sect. 15). This we
call the "small spiral".

4) With these values for the exceptional Green functions we
are now able to compute the right hand side of the renormalization
group equation for G_2, or rather Z^{-1}, from (14.15), using (14.20):

$$\frac{\mu\partial}{\partial\mu} \tilde{Z}_i^{-1}(\mu) = \tilde{Z}_i^{-1}(\mu) \left(\gamma_{ijk}g_j(\mu)g_k(\mu) + g^4(\mu)\textstyle\sum(\mu)\right) ,\tag{14.24}$$

where $\sum(\mu)$ is again bounded. Here γ_{ijk} are the one-loop γ coef-
ficients[14] This gives us *improved* propagators. See sect. (15.b).

5) Now we can compute the right hand side of eq. (14.4). Before integrating eq. (14.4) it is advisable to apply Ward identities (if we were dealing with a gauge theory) in order to reduce the number of independent degrees of freedom at each μ. As is well known, in gauge theories one can determine all subtraction constants this way except those corresponding to the usual free coupling constants and gauge fixing parameters[15]. So the number of unknown functions $g_i(\mu)$ need not exceed the number of "independent" coupling constants of the theory*.

6) Eq. (14.4) is now integrated, giving improved expressions for $g_i(\mu)$. Now go back to 2. This is the "second spiral", which will be seen to converge towards fixed values of $g_i(\mu)$.

The question of convergence of these two spirals is now discussed in the following section.

15. CONVERGENCE OF THE PROCEDURE

a) *Exceptional Momenta*

In sect. 13 a procedure is outlined to obtain the Green functions at exceptional momenta, if the Green functions at the symmetry point are given. That procedure is recursive because eqs. (13.4), (13.18), (13.22) and (13.25) determine the Green functions $G_{2,3,4}$ in terms of the symmetry ones, and $G_{4\mu}$, $G_{3\mu\nu}$, $G_{2\mu\nu\lambda}$. But the latter still contain the previous ansatz for $G_{2,3,4}$. Fortunately it is easy to show that any error $\delta G_{2,3,4}$ will reduce in size, so that here the recursive procedure converges:

Let us indicate the bounds discussed in sects. 5 and 13 as

$$|G_n(p_1,\ldots,p_n)| \leq B_n(p_1,\ldots,p_n) , \qquad (15.1)$$

and assume that a first trial $G_n^{(1)}$ has an error

$$|\delta G_n^{(1)}| \leq \varepsilon^{(1)} B_n , \qquad (15.2)$$

with some $\varepsilon^{(1)} \leq 2$.

Now $G_{4\mu}$, $G_{3\mu\nu}$, $G_{2\mu\nu\lambda}$ also satisfy inequalities of the form (15.1). Furthermore they were one order higher in g^2. So we have

---

* We put "independent" between quotation marks because our requirement of asymptotic freedom usually gives further relations among various running coupling constants, see appendix A

$$|\delta G_{4\mu}| \leqslant \varepsilon^{(1)} B_{4\mu} \sum_{n=4}^{\infty} n \, C^{n-2} g^{n-2} \, , \tag{5.3}$$

when the function $G_{4\mu}$ itself converges like

$$\sum c^n g^n \, ,$$

and $B_{4\mu}$ is the bound for $G_{4\mu}$ itself, as given by Table 2.

The procedure of sect. 13 can be applied unaltered to the error δG_n in the Green functions. But there is a factor in front,

$$\varepsilon^{(1)} \sum_{n=2}^{\infty} (n+2) \, c^n g^n = \varepsilon^{(2)} \, . \tag{15.4}$$

This gives for the newly obtained exceptional Green functions an error

$$|\delta G_n^{(2)}| \leqslant \varepsilon^{(2)} B \tag{15.5}$$

and $\varepsilon^{(2)} < \varepsilon^{(1)}$ if we reduce the maximally allowed value for g, as given by (5.9), somewhat more:

$$g_{max} \rightarrow 0.6527 \, g_{max} \, . \tag{15.6}$$

We stress that the above argument is only valid as long as the Green functions at their symmetry points were kept fixed and are determined by $g(\mu)$, bounded by (15.6).

b) *The Z Factors*

Knowing that at any stage $g(\mu)$ satisfies ineq. (14.9), we find that the solution of (14.24) is

$$\log \widetilde{Z}_i(\mu) = \int^{\mu} d \log \mu_1 (\gamma_{ijk} g_j(\mu_1) g_k(\mu_1) + g^4(\mu_1) \sum_i(\mu_1)) \, ;$$
$$\tag{15.7}$$

$$\widetilde{Z}_i(\mu) = \left(\log \frac{\mu}{\Lambda}\right)^{\sigma_i} (1+\mathcal{O}(g^2)) \, , \tag{15.8}$$

where the $\mathcal{O}(g^2)$ terms are again bounded by a coefficient times $g^2(\mu)$. These equations must be solved iteratively, because the right hand side of (15.7) contains skeleton expansions that again contain $Z(\mu)$, hidden in the function $\sum(\mu_1)$. It is not hard to convince oneself that such iterations converge. A change

$$|\delta Z| \leqq \varepsilon^{(1)} g^2 Z \tag{15.9}$$

yields a change in the function $\sum (\mu_1)$ bounded by

$$|\delta\textstyle\sum| \leqq \varepsilon^{(1)} g_0^2 \textstyle\sum , \tag{15.10}$$

so that

$$\frac{\delta\widetilde{Z}(\mu)}{\widetilde{Z}(\mu)} \leqq C\varepsilon^{(1)} g_0^2 g^2(\mu) \leqq \varepsilon^{(2)} g^2(\mu) \tag{15.11}$$

with $\varepsilon^{(2)} < \varepsilon^{(1)}$ if g_0 is small enough.

c) The coupling constants

We now consider the integro-differential equation (14.4). The solution is constructed iteratively by solving

$$\frac{\mu\partial}{\partial\mu} \widetilde{g}_i(\mu) + \sum_{\ell=2}^{k} \beta^{(\ell)}_{ij_1\ldots j_\ell} \widetilde{g}_{j_1}(\mu)\ldots\widetilde{g}_{j_\ell}(\mu) = |g(\mu)|^N \rho_i(\mu) , \tag{15.12}$$

where the tilde denotes the next "improved" function $g_i(\mu)$. Our first Ansatz will be a solution of (15.12) with $\rho_i\{g(\mu),\mu\}$ replaced by zero. This certainly exists because the β coefficients are determined by perturbation expansion and therefore finite. The integration constants must be chosen such that for all $\mu \geqslant m$ we have

$$|g(\mu)| \leqslant \kappa\, g_{max} \tag{15.13}$$

where g_{max} is the previously determined maximally allowed value of $g(\mu)$ and κ is again a constant smaller than 1 to be determined later. In practice this requirement implies asymptotic freedom[3]:

$$\lim_{\mu\to\infty} g(\mu) = o . \tag{15.14}$$

(It is constructive to consider also complex solutions.)

If we now substitute this $g(\mu)$ in the right hand side of eq. (15.12) we may find a correction:

$$g(\mu) \to g(\mu) = g(\mu) + \delta g(\mu) , \tag{15.15}$$

for which we may require

$$|\delta g(\mu)| \leqslant \varepsilon\, g_{max} \quad \text{for all } \mu . \tag{15.16}$$

We must start with:

$$\varepsilon + \kappa < 1 \tag{15.17}$$

Will a recursive application of eq. (15.12) converge to a solution? Let the first Ansatz produce a change (15.16). The next correction is then, up to higher orders in δg, given by

$$\frac{\mu \partial}{\partial \mu} \delta \tilde{g}_i(\mu) + M_{ij}(\mu) \delta \tilde{g}_j(\mu) = \delta f_i(\mu) \tag{15.18}$$

(where M_{ij} is determined by differentiation of (15.12) with respect to $g_i(\mu)$.

To estimate $\delta f(\mu)$ we must find a limit for the change in ρ. Our argument that $|\rho| < Q_N$ came from adding the absolute values of all diagrams contributing to ρ, possibly after application of (14.20) several times. Replacing (14.20) then by

$$|\delta g(\mu_1)| \leqslant \delta g(\mu) + 3c\left(\frac{\mu}{\mu_1}\right)^\varepsilon g^2(\mu) \delta g(\mu) \tag{15.19}$$

which indeed is true if g satisfies (15.18), or

$$\left|\frac{\mu \partial}{\partial \mu} \delta g\right| \leqslant 3\tilde{\beta} g^2 \delta g \ , \tag{15.20}$$

as can be derived from (14.20) and (14.21), we find that we can write

$$|\delta \rho| < \varepsilon C' \ , \tag{15.21}$$

with C' slightly larger than C, and

$$|\delta f(\mu)| \lesssim \varepsilon (N+1) C' g(\mu)^N \ . \tag{15.22}$$

Now asymptotically,

$$M_{ij}(\mu) \to M^0_{ij}/\log \mu \ , \tag{15.23}$$

where M^0_{ij} is determined by one-loop perturbation theory. If there is only one coupling constant it is the number 3/2. In the more general case we now assume it to be diagonalized:

$$M^0_{ij} = M(i)\delta_{ij} \ , \tag{15.24}$$

with one eigenvalue equal to 3/2. (Our arguments can easily be extended to the special situation when M^0_{ij} cannot be diagonalized, in which case the standard triangle form must be used.) The asymp-

totic form of the solution to (15.18) is

$$\delta g_i(\mu) = (\log \mu)^{-M(i)} \int_{\mu(i)}^{\mu} d \log \mu (\log \mu)^{M(i)} \delta f_i(\mu) , \qquad (15.25)$$

where $\mu(i)$ are integration constants. If $M(i) < \frac{N}{2} - 1$ then we choose $\mu(i) = \infty$. If $M(i) > \frac{N}{2} - 1$ we set $\mu(i) = m$. Then in both cases we get

$$|\delta \tilde{g}_i(\mu)| < \frac{\varepsilon(N+1)C''}{\left|\frac{N}{2} - M(i) - 1\right|} |g(\mu)|^{N-2} , \qquad (15.26)$$

where C'' is related to C' and the first β coefficient. In a compact set of μ values where the deviation from (15.25) is appreciable we of course also have an inequality of the form (15.16).

If $M(i) = N/2 - 1$ then we simply pick another N value (which needs not be integer here), raising or lowering it by one unit. We see that we only need to consider $N \leqslant 4$. Comparing (15.26) with (15.16), noting that C'' is independent of A, we see that if

$$\frac{(N+1)C''}{\left|\frac{N}{2} - M(i) - 1\right|} g_{max}^{N-3} < 1 \qquad (15.27)$$

then our procedure converges. Since C'' stays constant or decreases with decreasing g_{max}, we find that a finite g_{max} will satisfy (15.27).

Also we should check whether $\tilde{g}(\mu)$ satisfies the *Ansatz* (14.19), with unchanged $\tilde{\beta}$. This however is obvious from the construction of $\tilde{g}$ through eq. (15.18).
Notice that the masses are adjusted in every step of the iteration for the Z functions, by choosing A and B in section 14. They are necessary now because we wish to confine the integrals (15.25) at $\mu \geqslant m$, limiting the solutions $g(\mu)$ to satisfy $|g(\mu)| \leqslant g$.

16. BOREL SUMMABILITY[16]

The fact that we obtained eq. (14.4) holding for $m \leqslant \mu < \infty$ is our central result. For simplicity of the following discussions we ignore the *next-to-leading* terms of the coefficients β. Let us take the case that the leading ones have $\ell = 3$. We find that

$$g_i(\mu) = \frac{b_i^2}{\log \mu^2 + C} + \mathcal{O}(g^4(\mu)) \qquad (16.1)$$

(the next-to-leading β coefficients give an unimportant correction in the denominator of the form $\log \log \mu^2$). The coefficients b_i are fixed by the leading renormalization group β coefficients. We must choose C such that

$$|g^2(\mu)| \leqslant g^2_{max} \quad \text{if} \quad \mu \geqslant m .$$

(16.2)

This is guaranteed if either

$$\text{Re } C \gtrsim \frac{\max(b^2_i)}{g^2_{max}} - \log m^2 \equiv R - \log m^2$$

(16.3a)

or

$$|\text{Im } C| \gtrsim \frac{\max(b^2_i)}{g^2_{max}} \equiv R .$$

(16.3b)

Now the requirement of asymptotic freedom is usually so stringent that the constant C is the only free parameter besides the masses and possible dimension 1 coupling constants (a situation corresponding to the necessity of choosing all $\mu(i) = \infty$ in eq. (15.25)). But still we can do ordinary perturbation expansion, writing

$$g_i(m) = b_i g + \mathcal{O}(g^3) ;$$

(16.4)

$$C = \frac{1}{g^2} - \log m^2 .$$

(16.5)

where g is now a regular expansion parameter. The $\mathcal{O}(g^3)$ terms are fixed by the asymptotic freedom requirement and can be computed perturbatively. We now claim that perturbation expansion in g is indeed Borel-summable:

$$G(g^2) = \int_0^\infty F(z) e^{-z/g^2} dz ;$$

(16.6a)

$$F(z) = \frac{1}{2\pi i} \int_C G(g^2) e^{+z/g} d(g^{-2}) ,$$

(16.6b)

where the path C must be choosen to lie entirely in the region limited by eqs. (16.3) and (16.5) (see Fig. 17). Since in that region the Green functions $G(g^2)$ are approximately given by their perturbative values the integral (16.6b) will converge rapidly along this path, if
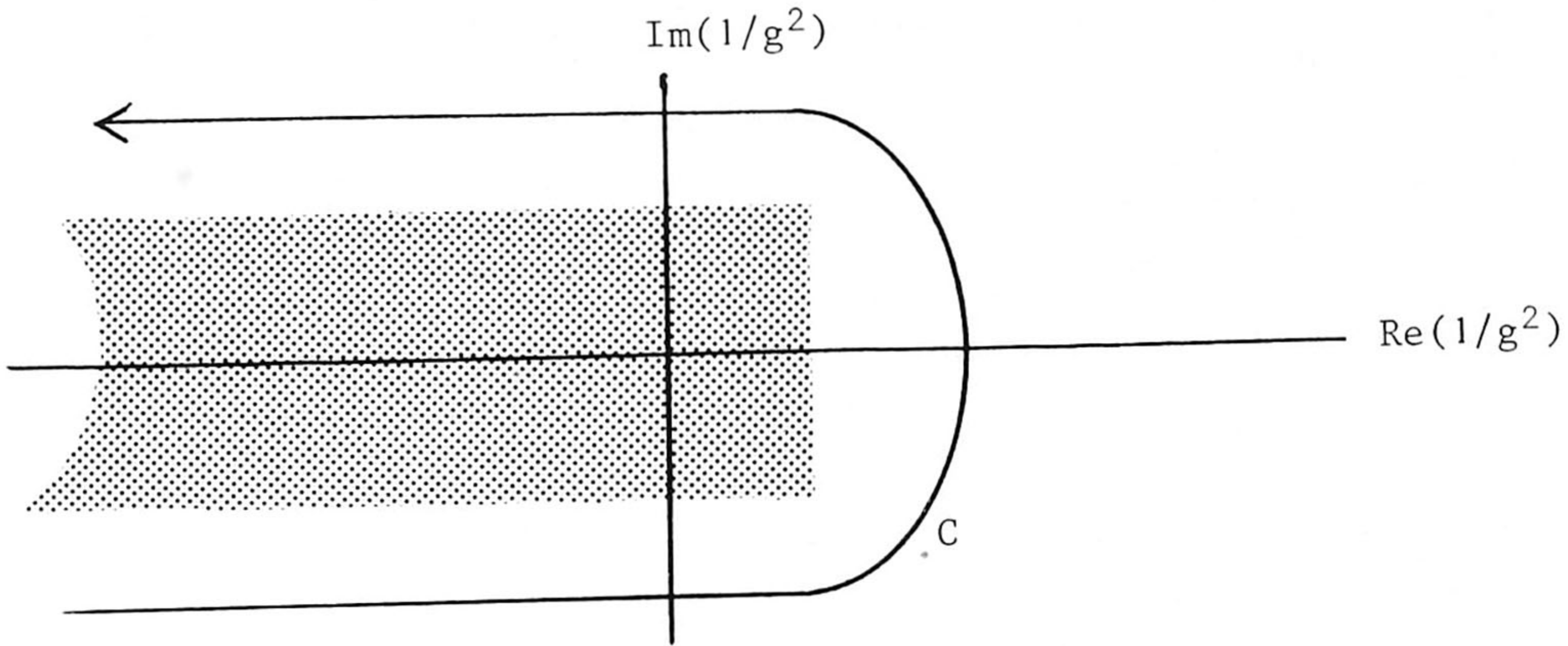
$$\text{Re } z > o ,$$

(16.7)

Fig. 17. The integration path C in eq. (16.7).

and F(z) will be bounded by

$$|F(z)| < A \exp(|z|/g_{max}^2) , \tag{16.8}$$

where g_{max} is the allowed limit for g as derived in the previous sections.

However, eqs. (16.7) and (16.8) are not quite sufficient to prove Borel summability because we also want to have analyticity of F(z) for an open region around the origin. That this requirement is met can be seen as follows. Let us solve a variant of equation (14.4) of the following form:

$$\frac{\mu \partial}{\partial \mu} g_i(\mu,\Lambda) = \left[- \sum_\ell \beta_{ij_1...j\ell}^{(\ell)} g_{j_1}(\mu,\Lambda)...g_{j\ell}(\mu,\Lambda) \right.$$
$$\left. + |g(\mu,\Lambda)|^N \rho_i(\mu,\{g\}) \right] \theta(\Lambda-\mu) , \tag{16.9}$$

where $\theta(x)$ is the step function. The coefficients $\beta^{(\ell)}$ and the functional ρ are the same as before (constructed the same way via difference equations of sects. 12 and 13). Clearly we have, if $\mu > \Lambda$: $g(\mu,\Lambda) = g(\Lambda,\Lambda)$. And eq. (16.1) now reads

$$g_i(\mu) = \frac{b_i^2}{\log \mu^2 + C} + \mathcal{O}(g^4(\mu)) ; \quad m \leqslant \mu \leqslant \Lambda . \tag{16.10}$$

Our point is that this solution exists not only in the region
(16.3), but also if

$$\text{Re } C \leqslant - \frac{\max(b_i)}{g^2_{\max}} - \log \Lambda^2 \equiv -R - \log \Lambda^2 \ .$$
(16.11)

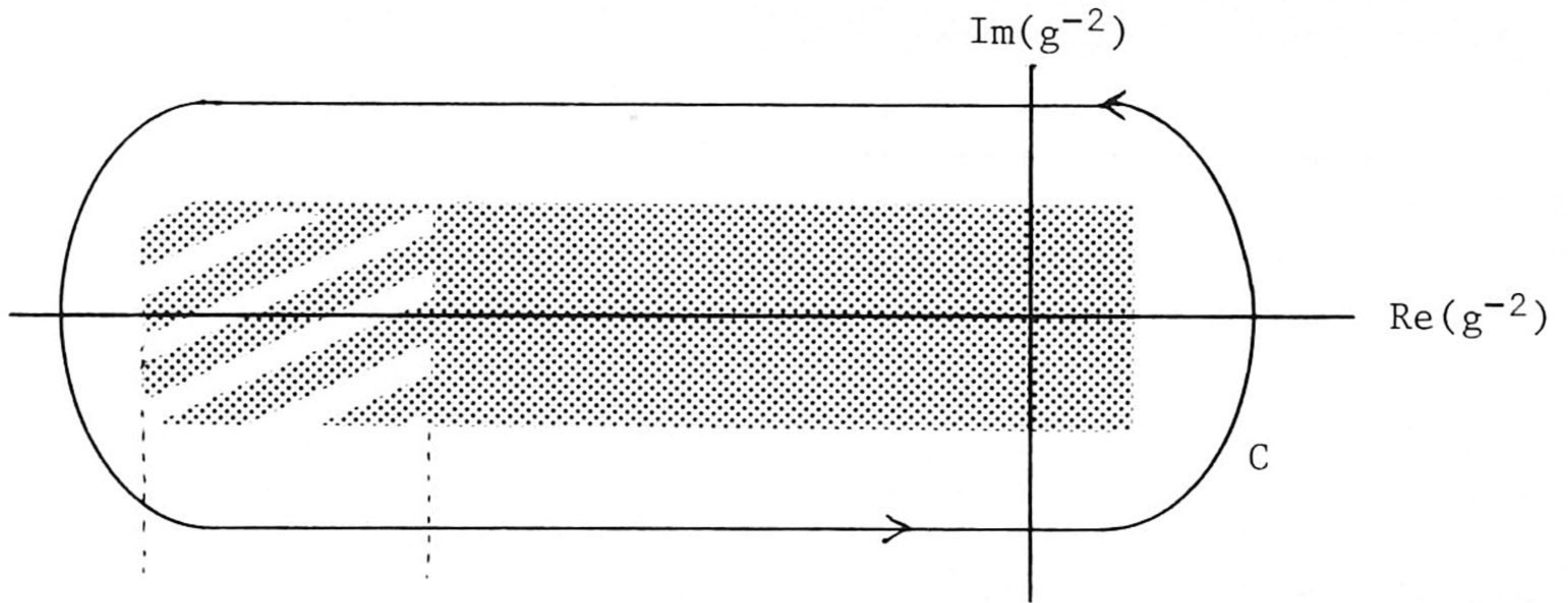We can now close the contour C (see Fig. 18).

Fig. 18. The contour C of eq. (16.13); the forbidden regions of
$G(g, \Lambda_i)$ are shaded.

$$-R - \log\left(\frac{\Lambda_2^2}{m^2}\right) \qquad -R - \log\left(\frac{\Lambda_1^2}{m^2}\right)$$

Now compare two different Λ values: Λ_1 and Λ_2, and compare the
Green functions computed with these two Λ values, both as a
function of g, taking

$$g_i(m, \Lambda) = b_i g + \mathcal{O}(g^3) \ .$$
(16.12)

We take these Green functions at (possibly exceptional) momentum
values p, but always such that $\Lambda \gg |p|$. If they are computed
directly following our algorithm then a slight Λ-dependence may
still exist, coming from two sources: one is the fact that
$g_i(\mu, \Lambda)$ depends on Λ because $\rho(\mu, \{g\})$ as a *functional* of g, may
depend on $g(\mu')$ with $\mu' > \Lambda$. But clearly, since all integrals
involved in the construction of ρ converge we expect this
dependence to go like

$$|\delta G| \lesssim \Lambda^{\varepsilon(g)-1}$$
(6.13a)

or probably

$$|\delta G| \underset{\sim}{\le} \Lambda^{\varepsilon(g)-2} \tag{16.13b}$$

(because linearly convergent equations can often be made
quadratically convergent by symmetrization); here $\varepsilon(g) \downarrow o$ if $g \to o$.
The second source of Λ-dependence comes from the application of
difference equations to compute Green functions away from the
symmetry point (sects. 12,13). Again, this error must behave like
(16.13), because of convergence of the integrals involved.

The change in the Borel function $F(z)$ can be read off from
eq. (16.6b)

$$\left| F(z,\Lambda_2) - F(z,\Lambda_1) \right| \underset{\sim}{\le} \frac{1}{2\pi i} \oint_C \Lambda_1^{\varepsilon(g)-2} e^{z/g^2} \, d(g^{-2}) \tag{16.14}$$

if $\Lambda_2 \underset{\sim}{\ge} \Lambda_1$.
Under what conditions does this vanish in the limit $\Lambda_1 \to \infty$? In our
integral g^{-2} ranges from $-R-\log\left(\frac{\Lambda_2^2}{m^2}\right)$ to R. So if $\mathrm{Re}\ z \le o$ then

$$\left| e^{z/g^2} \right| \underset{\sim}{\le} \left(\frac{\Lambda_2^2}{m^2} \, e^R \right)^{-\mathrm{Re}\,z} . \tag{16.15}$$

If $|g^{-2}| \to \infty$ then $\varepsilon(g) \downarrow o$. This we may use on the far left of the
curve C. Therefore ineq. (16.14) can be written as

$$|F(z,\Lambda_2) - F(z,\Lambda_1)| \underset{\sim}{\le} e^{R\left(\frac{\Lambda_2^2}{\Lambda_1^2}\right)} \Lambda_2^{-2\,\mathrm{Re}\,z-2} . \tag{16.16}$$

By comparing a series of Λ values of the form $\Lambda_n = 2^n$, one easily
sees that (16.16) guarantees convergence as soon as

$$\mathrm{Re}\ z > -1 , \tag{16.17}$$

which is a quite large region of analyticity of $F(z)$. Note that
$z = -1$ is the location of the first renormalon singularity[4],[7]. Eq.
(16.17) together with (16.8) implies complete Borel summability
of this theory.

17. THE MASSLESS THEORY

In the sections 14-16 the mass m^2 had to be non-zero. This
was the only way we could obtain the necessary ineq. (16.3a),
allowing us to draw the contour C. What happens if we take the
limit $m^2 \downarrow o$, considering not $g(m^2)$ but $g(\mu^2)$ at some fixed μ as

expansion parameter? Our method to construct the entire theory then fails, but for some z values $F(z)$ will still exist. The argument is analogous to the one of the previous section where we dealt with an ultraviolet problem. Now our difficulty is in the infrared. Comparing two different small values for m, we have

$$|\delta G| \underset{\sim}{\leq} (m^2)^{1-\varepsilon(g)} \; ; \tag{17.1}$$

$$|F(z,m_2) - F(z,m_1)| \underset{\sim}{\leq} \frac{1}{2\pi i} \oint_C (m_1^2)^{2-\varepsilon(g)} \, e^{z/g^2} \, d(g^{-2}) \; , \tag{17.2}$$

if $m_2 \underset{\sim}{<} m_1$.
Now if Re $z > 0$ then

$$\left| e^{z/g^2} \right| \underset{\sim}{\leq} \left(\frac{m^2}{\mu^2} e^R \right)^{Re\,z} . \tag{17.3}$$

Thus

$$|F(z,m_2) - F(z,m_1)| \underset{\sim}{\leq} e^R \left(\frac{m_1^2}{m_2^2} \right) m_2^{2-2Re\,z} . \tag{17.4}$$

Now we have convergence as $m^2 \downarrow 0$ as long as

$$Re \; z < 1 \; , \tag{17.5}$$

and, indeed, $z = 1$ is a point where an infrared renormalon singularity is to be expected. Thus, the Borel transform $F(z)$ of the massless theory is analytic in the region

$$-1 < Re\,z < 1 \; . \tag{17.6}$$

This result guarantees that perturbation expansion in g^2 diverges not worse than

$$g^{2n} \, n!$$

but is clearly not enough for Borel summability.

18. THE $-\lambda \, Tr \, \phi^4$ MODEL

A special case is the pure scalar planar field theory, with just one coupling constant λ and a mass m. If m is sufficiently large and λ sufficiently small then our analysis applies, and we find that all planar Green functions are uniquely determined. However, in this special case there is more: the Green functions can be uniquely determined as long as the masses in *all* channels

are non-negative, and λ is negative. This was discovered by comparing with the much simpler "spherical model" (appendix B) which shows the same property.

The argument is fairly simple. Let us first take the theory at m^2 values which are so large that everything is well-defined. Now decrease the "bare mass" m_B^2 continuously. The change in the dressed propagator

$$P(k,m^2) = -G_2^{-1}(k,m^2) \tag{18.1}$$

is determined by

$$\frac{\partial}{\partial m^2} G_2(k,m^2) \equiv G'(k,m^2) \tag{18.2}$$

which we take to start out at sufficiently large m^2.

Now the Feynman rules for

$$G''(k,m^2) \equiv \frac{\partial}{\partial m^2} G'(k,m^2) , \tag{18.3}$$

can easily be written down, just like those for

$$\frac{\partial}{\partial m^2} G_4(k_1,\ldots,k_4,m^2) \equiv G_4' . \tag{18.4}$$

Since G_2'' and G_4' are superficially convergent we can again express them in terms of a skeleton expansion containing only the functions G_4 and $-G_2$ and the propagators P. *They are all positive* (remember that G_4 starts out as $-\lambda$, with $\lambda < 0$), *and all integrals and summations converge.* Only G_4' has one surviving minus sign from differentiating one propagator with m . Thus:

$$G_2'' > 0 ; \tag{18.5}$$

$$G_4' < 0 . \tag{18.6}$$

If we let m^2 decrease then clearly G_2 will stay positive and G_2' negative. Their absolute values grow however, until a point is reached where either the sum of all diagrams will no longer converge, or the two-point function G_2 becomes zero. As soon as this happens the theory will be ill-defined. A tachyonic pole tends to develop, followed by catastrophes in all channels. The point we wish to make in this section however is that as long as this does not happen, indeed all summations and integrals converge, so that our iterative procedure to produce the Green functions will also converge. For all those values of λ and m^2 this theory will be Borel summable.

This result only holds for the special case considered here, namely $-\lambda \operatorname{Tr} \phi^4$ theory, because all skeleton diagrams that con-

tribute to some Green function, carry the same sign. They can never interfere destructively.

Notice that what also was needed here was convergence of the diagram expansion. Now we know that at finite N the non-planar graphs give a divergent contribution. Thus the "tachyons" will develop already at infinite m^2: the theory is fundamentally unstable. Of course we knew this already: λ after all has the wrong sign. The instantons that bring about the decay of our "false vacuum" carry on action S proportional to $-N/\tilde{\lambda}$ which is finite for finite N.

19. OUTLOOK

Apart from the model of sect. 18, the models we are able to construct explicitly now lack any appreciable structure, so they are physically not very interesting. Two (extremely difficult) things should clearly be tried to be done: one is the massless planar theories such as SU(∞) QCD. Clearly that theory should show an enormously intricate structure, including several possible phase-transitions. We still believe that more and better understanding of the infrared renormalons that limited analyticity of our borel functions in sect. 17 could help us to go beyond those singular points and may possibly "solve" that model (i.e. yield a demonstrably convergent calculational scheme).

Secondly one would try to use the same or similar skeleton techniques at finite N (non-planar diagrams). Of course now the skeleton expansion does not converge, but, in Borel-summing the skeleton expansion there should be no renormalons, and all divergences may be due entirely to instantonlike structures. More understanding of resummation techniques for these diagrams by saddle point methods could help us out. If such a program could work then that would enable us to write down SU(3) QCD in a finite (but small) box. QCD in the real world could then perhaps be obtained by gluing boxes together, as in lattice gauge theories.

Another thing yet to be done is to repeat our procedure now in Minkowsky space instead of Euclidean space. Singling out the obvious singularities in Minkowsky space may well be not so difficult, so perhaps this is a more reasonable challenge that we can leave for the interested student.

APPENDIX A. ASYMPTOTICALLY FREE INFRARED CONVERGENT PLANAR HIGGS MODEL

In discussing examples of planar field theories for which our analysis is applicable we found that pure SU(∞) gauge theory (with possibly a limited number of fermions) is asymptotically free as required, but unbounded in the infrared – so that even the ultraviolet limit cannot be treated exactly (see sects. 14 and 15).

$-\lambda \, \text{Tr} \, \varphi^4$ is asymptotically free and can be given a mass term
so that infrared convergence is also guaranteed. At $N \to \infty$ this is
a fine planar theory, but at finite N the vacuum is unstable. The
only theory that suffers from none of these defects is an $SU(\infty)$
gauge theory in which all bosons get a mass due to the Higgs
mechanism. But then a new scalar self-coupling occurs that tends
to be not asymptotically free. Asymptotic freedom is only secured
if, curiously enough, several kinds of fermionic degrees of
freedom are added. The following model is an example (similar
examples can also be constructed at finite N, such as SU(2)).

In general a renormalizable model can be written as

$$\mathcal{L} = - \tfrac{1}{4} G^a_{\mu\nu} G^a_{\mu\nu} - \tfrac{1}{2}(D_\mu \phi_i)^2 - V(\phi_i) - \bar{\psi}(\gamma D + W(\phi))\psi \,, \tag{A.1}$$

where G is the covariant curl, ϕ_i is a set of scalar fields and ψ
a set of spinors. V is a quartic and W a linear polynomial in ϕ.
We write

$$G^a_{\mu\nu} = \partial_\mu A^a_\nu - \partial_\nu A^a_\mu + g^{abc} A^b_\mu A^c_\nu$$

$$D_\mu \phi_i = \partial_\mu \phi_i + T^a_{ij} A^a_\mu \phi_j$$

$$D_\mu \psi_i = \partial_\mu \psi_i + U^a_{ij} A^a_\mu \psi_j$$

$$W = S + iP\gamma_5 \;;\; \hat{W} = S - iP\gamma_5$$

$$U = U_s + U_p \gamma_5 \;;\; \hat{U} = U_s - U_p \gamma_5$$

$$C_1^{ab} = g^{apq} g^{bpq} \;;\; C_2^{ab} = -\text{Tr} \, T^a T^b$$

$$C_3^{ab} = -\text{Tr}\left(U_L^a U_L^b + U_R^a U_R^b\right) = -2\text{Tr}\left(U_s^a U_s^b + U_p^a U_p^b\right) \,. \tag{A.2}$$

The most compact way to write the complete set of one-loop β
functions is to express them in terms of the one-loop counter-
Lagrangian, $[8\pi^2(4-n)]^{-1}\Delta\mathcal{L}$, where $\Delta\mathcal{L}$ has been found to be[17], after
performing the necessary field renormalizations,

$$\Delta\mathcal{L} = G^a_{\mu\nu} G^b_{\mu\nu}\left[\frac{11}{12} C_1^{ab} - \frac{1}{24} C_2^{ab} - \frac{1}{6} C_3^{ab}\right]$$

$$+ \frac{1}{4} V_{ij}^2 + \frac{3}{2} V_i (T^2\phi)_i + \frac{3}{4}(\phi T^a T^b \phi)^2$$

$$+ \bar{\psi}\left\{\frac{1}{4} W_i \hat{W}_i W + \frac{1}{4} W \hat{W}_i W_i + W_i \hat{W} W_i\right\}\psi$$

$$+ \frac{3}{2} \bar{\psi}(\hat{U}^2 W + W U^2)\psi + \phi_i (V_j + \bar{\psi} W_j \psi)\text{Tr}(S_i S_j + P_i P_j)$$

$$- \text{Tr}(S^2 + P^2) + \text{Tr}[S,P]^2 \,. \tag{A.3}$$

Here V_i stands for $\partial V/\partial \varphi_i$, etc.

The scaling behavior of the coupling constants is then determined by

$$\frac{\mu \partial \mathcal{L}}{\partial \mu} = -\frac{\Delta \mathcal{L}}{8\pi^2} . \tag{A.4}$$

We now choose a model with $U(N)_{local} \times SU(N)_{global}$ symmetry. Besides the gauge field we have a scalar ϕ_i^s in the $N_{local} \times N_{global}$ representation, and two kinds of fermions:

$\psi_{(1)i}{}^j$ in $N_{local} \times N_{local}$ and $\psi_{(2)a}{}^i$ in $N_{local} \times N_{global}$. We choose

$$V(\phi) = \frac{\lambda}{2} \phi_i^{*s} \phi_i^t \phi_j^{*t} \phi_j^s , \tag{A.5}$$

and

$$\bar{\psi} W \psi = h \left[\bar{\psi}_{(2)}{}^a{}_i \phi_a^{*j} \psi_{(1)j}{}^i + h.c. \right] . \tag{A.6}$$

Writing

$$C_1^{ab} = C_2^{ab} = \tilde{g}^2 \delta^{ab} ; \quad C_3^{ab} = 3\tilde{g}^2 \delta^{ab} , \tag{A.7}$$

we find:

$$-8\pi^2 \frac{\mu \partial \tilde{g}^2}{\partial \mu} \equiv \Delta \tilde{g}^2 = \frac{3}{2} \tilde{g}^4 ; \tag{A.8}$$

and with $\tilde{\lambda} \equiv N\lambda$; $\tilde{h}^2 = Nh^2$, by substituting (A.5) and (A.6) in the expression (A.3) after some algebra, and in the limit $N \to \infty$:

$$\Delta \tilde{h}^2 = -3\tilde{h}^4 + \frac{9}{2} \tilde{h}^2 \tilde{g}^2 ; \tag{A.9}$$

$$\Delta \tilde{\lambda} = -2\tilde{\lambda} + 3\tilde{g}^2 \tilde{\lambda} - \frac{3}{4} \tilde{g}^4 - 4\tilde{h}^2 \tilde{\lambda} + 4\tilde{h}^4 . \tag{A.10}$$

These equations (A.8)-(A.10) are ordinary differential equations whose solutions we can study. The signs in all terms are typical for any such models with three coupling constants g, λ and h. Only the relative magnitudes of the various terms differ from one model to another. For asymptotic freedom we need that the second and last terms of (A.10) and the last of (A.9) are sufficiently large. Usually this implies that the fermions must be in a sufficiently large representation of the gauge group, which explains our choice for the fermionic representations. Our model has an asymptotically free solution if all coupling constants stay in a fixed ratio with respect to each other:

$$\tilde{\lambda} = \hat{\lambda} \tilde{g}^2 ; \quad \tilde{h} = \hat{h} g , \tag{A.11}$$

and then, from (A.8)-(A.10) we see:

$$\hat{h} = 1 \; ;$$

$$\hat{\lambda} = \frac{1}{8} (\sqrt{129}-5) \; . \tag{A.12}$$

So indeed we have a solution with positive λ.

It now must be shown that in this model all particles can be made massive via the Higgs mechanism. We consider spontaneous breakdown of $SU(N)_{local} \times SU(N)_{global}$ into the diagonal $SU(N)_{global}$ subgroup. Take as a mass term

$$-\mu \; \phi_i^{*s} \; \phi_i^s \; . \tag{A.13}$$

We can write V as

$$V = \frac{\lambda}{2} \left| \phi_i^{*s} \; \phi_i^t - F^2 \delta^{st} \right|^2 + \text{const.} \tag{A.14}$$

Clearly this is minimal if

$$\phi_i^s = F\delta_i^s \; , \tag{A.15}$$

or a gauge rotation thereof.
All vector bosons get an equal mass:

$$-D^*\phi \; D\phi \Rightarrow - g^2 F^2 A_\mu^2 \; ; \tag{A.16}$$

$$M_A^2 = 2g^2 F^2 \; , \tag{A.17}$$

and of course the scalars get a mass:

$$M_H^2 = \lambda F^2 \; . \tag{A.18}$$

Thus the mass ratio is given by

$$\sqrt{\hat{\lambda}/2} = 0.6303 \quad 6778\ldots \; . \tag{A.19}$$

This is a fixed number of this theory, but it will be affected by higher order corrections. The fermions can each be given a mass term:

$$- m_1 \bar{\psi}_{(1)} \psi_{(1)} - m_2 \bar{\psi}_{(2)} \psi_{(2)} \; , \tag{A.20}$$

and the Yukawa force will give a mixing of a definite strength. The model described in this Appendix is probably the simplest completely convergent planar field theory with absolutely stable vacuum. It is unlikely however that it would have a direct physical significance.

APPENDIX B. THE N-VECTOR MODEL IN THE N → ∞ LIMIT (SPHERICAL MODEL). SPONTANEOUS MASS GENERATION

When only N-vector fields are present (rather than N×N tensors) then the $N \to \infty$ limit is easily obtained analytically. This is the quite illustrative spherical model. Let the bare Lagrangian be

$$\mathcal{L} = -\tfrac{1}{2}(\partial_\mu \vec{\phi})^2 - \tfrac{1}{2}m_B^2 \vec{\phi}^2 - \frac{\lambda_B}{8}(\vec{\phi}^2)^2 .$$

(B.1)

The only diagrams that dominate in the $N \to \infty$ limit are the chains of bubbles (Fig. 19).
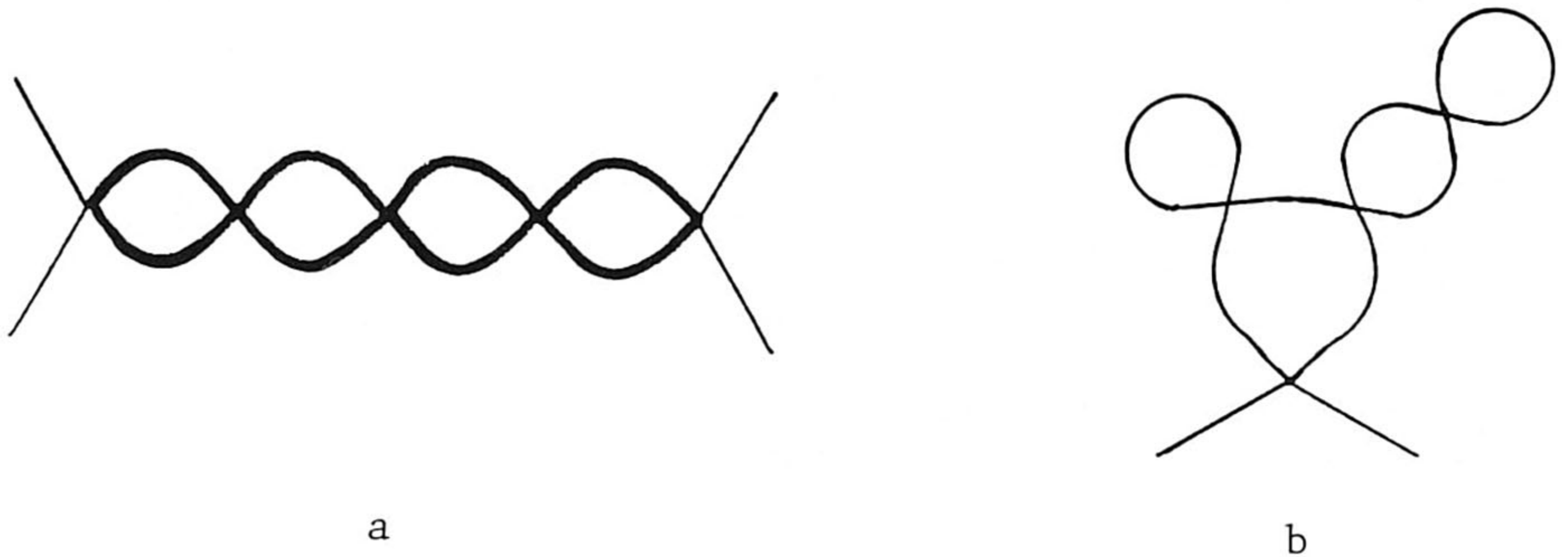
a

b

Fig. 19. a) Dominating diagrams for the 4-point function. b) Mass renormalization.

Let us remove some factors π^2 by defining

$$\tilde{\lambda}_B = N\lambda_B / 16\pi^2 .$$

(B.2)

The diagrams of Fig. 19 are easily summed. Mass and coupling constant need to be renormalized. Dimensional renormalization is appropriate here. In terms of the finite constants $\tilde{\lambda}_R(\mu)$ and $m_R(\mu)$, chosen at some subtraction point μ, and the infinitesimal $\varepsilon = 4-n$, where n is the number of space-time dimensions, one finds:

$$\tilde{\lambda}_B = -\varepsilon\left(1 + \frac{\varepsilon}{\tilde{\lambda}_R(\mu)}\right)\mu^\varepsilon ,$$

(B.3)

and

$$m_B = \mu m_R(\mu)\sqrt{\frac{-\varepsilon}{\tilde{\lambda}_R(\mu)}} .$$

(B.4)

The sum of all diagrams of type 19a gives an effective propagator of the form

$$F(q) = \frac{32\pi^2/N}{\gamma - \dfrac{2}{\tilde{\gamma}_R(\mu)} + \log \dfrac{\pi m^2}{\mu^2} + f(\dfrac{q^2}{m^2}) - i\varepsilon} \quad , \tag{B.5}$$

where q is the exchanged momentum, γ is Euler's constant, and

$$f(\frac{q^2}{m^2}) = \int_0^1 dx \, \log\left|1 + \frac{x(1-x)q^2}{m^2}\right| - \pi i \theta(-q^2 - 4m^2)\sqrt{1 + \frac{4m^2}{q^2}} \quad , \tag{B.6}$$

and m is the *physical* mass in the propagators of Fig. 19a; that is because these should include the renormalizations of the form of Fig. 19b.

Fig. 20.

Fig. 20 shows how m follows from m_R:

$$2m_R^2\mu^2 = \tilde{\lambda}_R m^2 \, \log\left(\frac{\pi m^2}{\mu^2} + \gamma - 1 - \frac{2}{\tilde{\lambda}_R}\right) = 0 \quad . \tag{B.7}$$

From (B.3) we see that the renormalization-group invariant combination is

$$\frac{1}{\tilde{\lambda}_R(\mu)} + \log\mu \quad , \tag{B.8}$$

so that inevitably $\tilde{\lambda}_R < 0$ at large μ. Indeed, in this model the vacuum would become unstable as soon as N is made finite. In the limit $N \to \infty$ however everything is still fine.

Now in Fig. 21 we plot both m_R^2 and the composite mass M^2, determined by the pole of $F(q)$, as a function of the physical mass m^2. We see that at negative m_R^2 there are two solutions for m^2, but one should be rejected because M^2 would be negative, an indication for an unstable choice of vacuum.
The observation we wish to make in this appendix is that in the allowed region for m_R^2 we get an entirely positive 4-point function in Euclidean space ($F(q) > 0$). If we chose m_R^2 to be fixed and vary $\tilde{\lambda}_R$ (or rather vary $\tilde{\lambda}_B$) then at $m_R^2 \geq 0$ *all* $\tilde{\lambda}$ values are allowed, at negative m_R^2 only sufficiently small values. At $m_R^2 = 0$ we see a
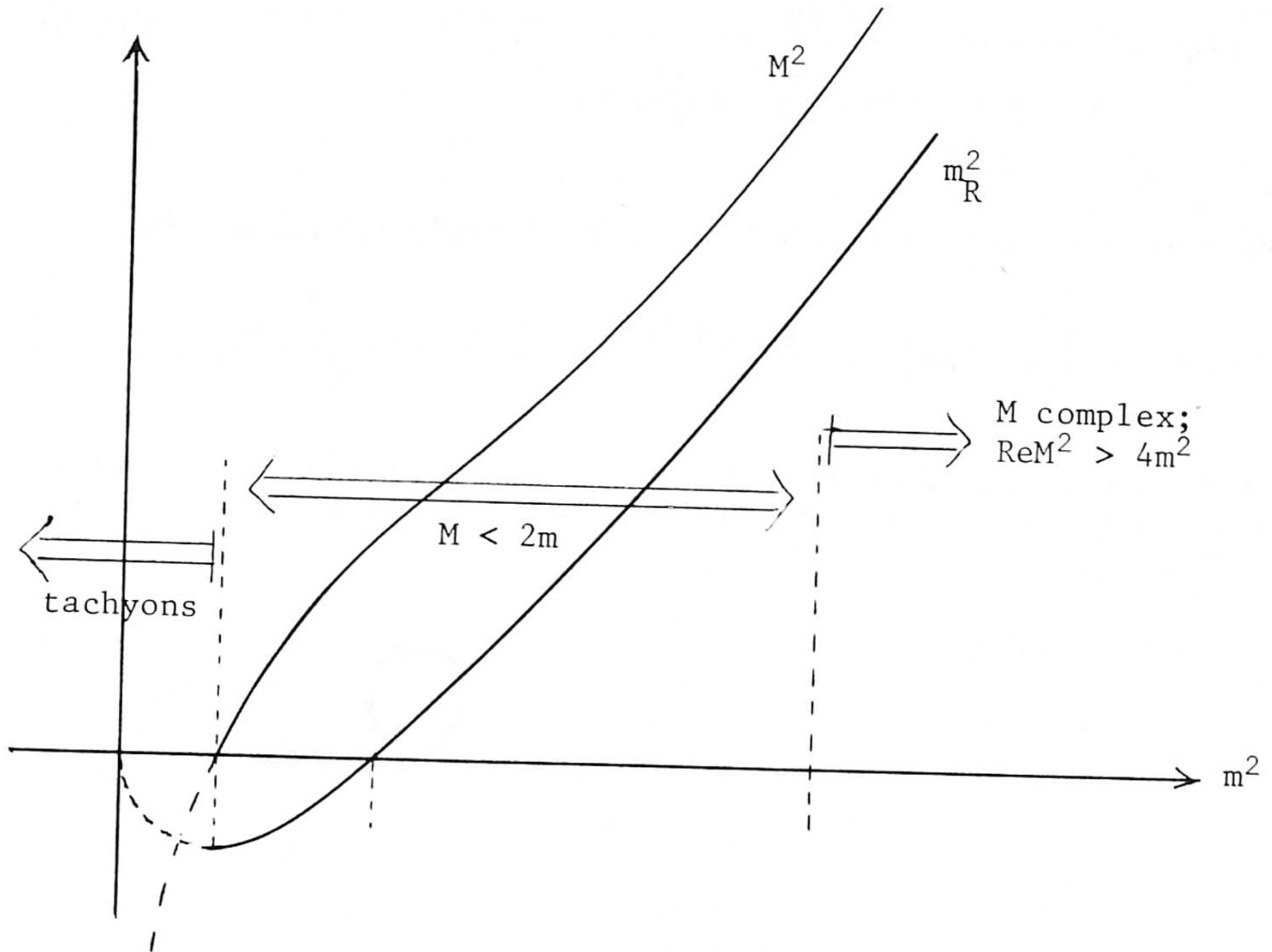
Fig. 21. Mass ratios at given value for $\tilde{\lambda}_R(\mu)$.

"spontaneous" generation of a finite value for m . Perturbation expansion in λ_R would show the "infrared renormalon" difficulty. Apparently here the difficulty solves itself via this spontaneous mass generation.

REFERENCES

1. E.C.G. Stueckelberg and A. Peterman, Helv. Phys. Acta 26 (1953), 499; M. Gell-Mann and F. Low, Phys. Rev. 95 (1954) 1300.
2. K.G. Wilson, Phys. Rev. D10, 2445 (1974).
   K.G. Wilson, in "Recent Developments in Gauge Theories", ed. by G. 't Hooft et al., Plenum Press, New York and London, 1980, p. 363.
3. G. 't Hooft, Marseille Conference on Renormalization of Yang-Mills Fields and Applications to Particle Physics, June 1972, unpublished; H.D. Politzer, Phys. Rev. Lett. 30, 1346 (1973); D.J. Gross and F. Wilczek, Phys. Rev. Lett. 30, 1343 (1973).
4. G. 't Hooft, in "The Whys of Subnuclear Physics", Erice 1977, A. Zichichi ed. Plenum Press, New York and London 1979, p. 943.
5. M. Creutz, L. Jacobs and C. Rebbi, Phys. Rev. Lett. 42, 1390 (1979).
6. C. de Calan and V. Rivasseau, Comm. Math. Phys. 82, 69 (1981); 91, 265 (1983).

7) G. Parisi, Phys. Lett. 76B, 65 (1978) and Phys. Rep. 49, 215 (1979).
8) J. Koplik, A. Neveu and S. Nussinov, Nucl. Phys. B123, 109 (1977).
   W.T. Tuttle, Can. J. Math. 14, 21 (1962).
9) See ref. 3.
10) J.D. Bjorken and S.D. Drell, Relativistic Quantum Mechanics (McGraw-Hill, New York, 1964).
11) G. 't Hooft, Commun. Math. Phys. 86, 449 (1982).
12) G. 't Hooft, Commun. Math. Phys. 88, 1 (1983).
13) J.C. Ward, Phys. Rev. 78 (1950) 1824.
   Y. Takahashi, Nuovo Cimento 6 (1957) 370.
   A. Slavnov, Theor. and Math. Phys. 10 (1972) 153 (in Russian). English translation: Theor. and Math. Phys. 10, p. 99.
   J.C. Taylor, Nucl. Phys. B33 (1971) 436.
14) K. Symanzik, Comm. Math. Physics 18 (1970) 227; 23 (1971) 49; Lett. Nuovo Cim. 6 (1973) 77; "Small-Distance Behaviour in Field Theory", Springer Tracts in Modern Physics vol. 57 (G. Höhler ed., 1971) p. 221.
15) G. 't Hooft, Nucl. Phys. B33 (1971) 173.
16) G. 't Hooft, Phys. Lett. 119B, 369 (1982).
17) G. 't Hooft, unpublished.
   R. van Damme, Phys. Lett. 110B (1982) 239.